MICROBIAL INACTIVATION BY COPPER-BASED DISINFECTION SYSTEMS: EFFICACY AND MECHANISM

Hyung-Eun Kim

Department of Urban and Environmental Engineering
(Environmental Science and Engineering)

Graduate School of UNIST

Microbial inactivation by copper-based disinfection systems: Efficacy and mechanism

A dissertation
submitted to the Graduate School of UNIST
in partial fulfillment of the
requirements for the degree of
Doctor of Philosophy

Hyung-Eun Kim

01/16/2017 of submission

Approved by

Advisor
Changha Lee

Microbial inactivation by copper-based disinfection systems: Efficacy and mechanism

Hyung-Eun Kim

This certifies that the dissertation of Hyung-Eun Kim is approved.

01/16/2017 of submission

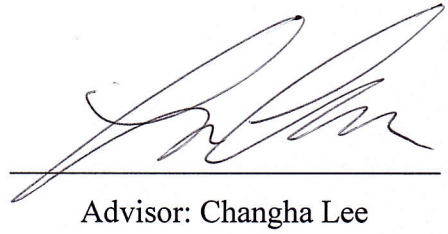

Advisor: Changha Lee

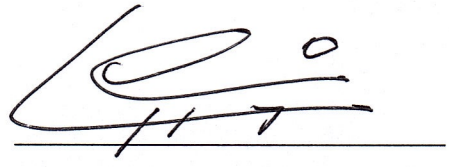

Jaeweon Cho

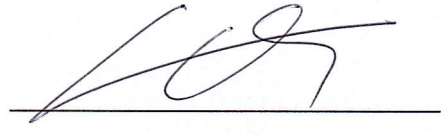

Changsoo Lee

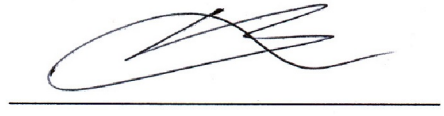

Min Cho

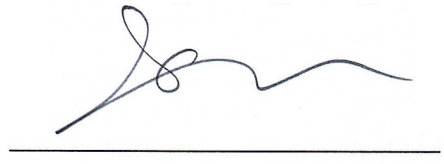

Yunho Lee

ABSTRACT

To control the pathogenic microorganisms threatening human health in drinking water, it is important to utilize proper physical or chemical disinfection processes at drinking water treatment plants. Various methods have been studied to efficiently control the microorganisms in water. While conventional chemical disinfectants, such as chlorine or ozone, are effective, by-products are produced, depending upon the water quality. However, metals, which are essential nutrient elements, exhibit antimicrobial properties, both to bacteria and viruses. Copper, which has been studied as an effective antibacterial, antiviral, and antifungal reagent, was selected in this work. In this study, *E. coli* and MS2 coliphage, the surrogates of bacteria and viruses, respectively, were treated by homogeneous or heterogeneous copper-based disinfection systems.

The inactivation of *E. coli* and MS2 coliphage by Cu(II) is found to be significantly enhanced in the presence of hydroxylamine (HA). The addition of a small amount of HA (i.e., 5–20 μM) increased the inactivation efficacies of *E. coli* and MS2 coliphage by 5- to 100-fold, depending on the conditions. Dual effects were anticipated to enhance the biocidal activity of Cu(II) by the addition of HA, viz. i) the accelerated reduction of Cu(II) into Cu(I) (a stronger biocide) and ii) the production of reactive oxidants from the reaction of Cu(I) with dissolved oxygen (evidenced by the oxidative transformation of methanol into formaldehyde). Deaeration enhanced the inactivation of *E. coli* but slightly decreased the inactivation efficacy of MS2 coliphage. The addition of 10 μM hydrogen peroxide (H_2O_2) greatly enhanced the MS2 inactivation, whereas the same concentration of H_2O_2 did not significantly affect the inactivation efficacy of *E. coli.* Observations collectively indicate that different biocidal actions lead to the inactivation of *E. coli* and MS2 coliphage. The toxicity of Cu(I) is dominantly responsible for the *E. coli* inactivation. However, for the MS2 coliphage inactivation, the oxidative damage induced by reactive oxidants is as important as the effect of Cu(I).

The Cu(II) and PMS combined system was examined to inactivate *E. coli* and MS2 coliphage in natural water. PMS is emerging oxidants commonly applied to the in situ treatment of organic contaminations for waste water and ground water. PMS is activated by the transition metal such as Co(II), Fe(II), Ni(II), producing sulfate radical or hydroxyl radical. In this study, the combined system varying the concentration of PMS with fixed Cu(II) concentration of 0.01 mM, exhibited a synergistic effect on both *E. coli* and MS2 coliphage inactivation in natural water. The presence of hydroxyl radical scavengers marginally inhibited the inactivation rate of the Cu(II)/PMS system,

however, that presence almost inhibited the copper-chelating reagents, EDTA and DMP. The Cu(II)/PMS system is assumed to generate reactive oxidants rather than hydroxyl radical, and most reactive oxidants are due to the Cu(II) ion. Most reactive oxidants produced intracellular rather than extracellular region that is more lethal to *E. coli*. In particular, when *E. coli* was exposed to Cu(II) first, the sequential addition showed the highest efficacy. Thus, it is worth consideration to add sequentially for more effective application of the Cu(II)/PMS system.

The biocidal effects of iron-based bimetallic nanoparticle, nFeCu, were tested to inactivate *E. coli* and MS2 coliphage, surrogate of bacteria and virus, respectively, and the mechanisms of production of the biocidal reagents were elucidated. In this study, nFeCu was synthesized via ferric ion reduction using sodium borohydride followed by the displacement of copper ion. The nFeCu showed enhanced biocidal effects compare to the single composite nanoparticles, nFe and nCu. nFeCu showed different inactivation mechanisms on *E. coli* and MS2 coliphage. In the absence of oxygen, the *E. coli* inactivation efficiency was greater than that observed in the presence of oxygen. In contrast to the *E. coli* inactivation results, MS2 coliphage inactivation was nearly inhibited in the presence of oxygen. nFeCu is assumed to generate Cu(I), which is a strong biocides, via a copper-catalyzed Fenton-like reaction and to produce reactive oxidants, such as $^{\bullet}OH$, Fe(IV) or Cu(III), from the Fenton or Fenton-like reaction with in situ generated H_2O_2. The *E. coli* inactivation efficiency was lowered more by the nCu/H_2O_2 system than by nFeCu, and was inhibited by the increase of H_2O_2 concentration. However, the MS2 coliphage inactivation efficiency was enhanced by the increase of H_2O_2 concentration; further, the higher concentration of H_2O_2 dramatically enhanced the inactivation rate. We concluded the *E. coli* inactivation was more likely induced by Cu(I) damaging culturability, rather than membrane damage. Meanwhile, the reactive oxidants produced by nFeCu exhibited oxidative damage on the culturability and antigenicity of MS2 coliphage.

CONTENSTS

List of Figures

List of Tables

CHAPTER 1.

Overview

1.1. Antimicrobial effect of metal (metal toxicity)

The public health risk from waterborne diseases caused by pathogenic microorganisms has continuously raised concerns, and has promoted research on drinking water disinfection. Among the disinfection technologies suggested, chemical disinfectants are found to be effective for inactivating a broad spectrum of microorganisms, and are therefore widely used for various water disinfection applications.

Metals, such as Na, Mg, K, Ca, Mn, Fe, Co, Ni, Cu and Zn, are normally required for living microorganisms. They are necessary to maintain various enzymatic functions and metabolism processes in the cells and the formation of structures. However, when the concentration is excessive, these metals can be lethal to microorganisms. The antimicrobial effects of metal (or metal toxicity) have therefore been widely studied, but metal-induced biocidal action has remained unclear. Recent studies have reported that different metals cause microbial damage as a result of oxidative stress, or protein or membrane damage (Dizaj et al., 2014, Lemire et al., 2013). Metals primarily bind to microorganisms such as thiol and other groups on protein, or enzymes. Metals also bind to the DNA or RNA and disrupt, or accumulate inside involving metabolism mechanisms (Sterritt and Lester, 1980). Common mechanisms involving the Fenton reaction generate the superoxide radical and the hydroxyl radical involved iron or copper.

1.2. Antimicrobial effects of copper

Copper is not only a ubiquitous metal in the technological environment, it is also essential for the function of most living organisms. In addition, copper has common valences of +2 or +1, so the ions may be involved in electron-transfer processes (Bondarenko et al., 2013). It has potential as a disinfectant that does not produce disinfectant by-products (DBPs) like chlorine or ozone, which are human carcinogens. Unlike other chemical disinfectants, copper ions may remain in the water for a long time, and have a larger residual effect. Moreover, copper can be immobilized in various ways,

and ions that are released from surfaces and are bounded to surface will take part in the inactivation of microorganisms.

Several mechanisms have been reported to explain Cu-induced toxicity. Both Cu(I) and Cu(II) ions can participate in oxidation and reduction reactions that contribute to lethal action (Beswick et al., 1976, Kimura and Nishioka, 1997, Kirakosyan et al., 2008, Park et al., 2012, Stohs and Bagchi, 1995). Combination with auxiliary compounds such as hydrogen peroxide (H_2O_2), improved the biocidal activity of Cu(II) was improved to a significant extent, exhibiting distinctive biocidal activity on a wide spectrum of viruses (i.e., single- and double- stranded DNA and RNA viruses) (Nieto-Juarez et al., 2010, Patikarnmonthon et al., 2010, Sagripanti et al., 1993, Yamamoto et al., 1964). Due to their chemical and physical properties, copper and copper oxide nanoparticles have been focused on as antimicrobial materials. These are effective against gram-positive and gram-negative bacteria with high stability, and are also applicable for antifungal activity (Mahapatra et al., 2008, Azam et al., 2012).

1.2.1. Copper ions

Cupric ion (Cu(II)) is a chemical disinfectant that has been extensively studied for its antimicrobial activity. It has been reported that Cu(II) is effective in inactivating bacteria (Park et al., 2012, Volentini et al., 2011), viruses (Borkow et al., 2007, Nieto-Juarez et al., 2010, Sagripanti et al., 1993), yeast cells (Ohsumi et al., 1988), daphnia (de Schamphelaere and Janssen, 2002), and algae (Crist et al., 1988), but it has minor effects on inactivation of viruses (Sagripanti et al., 1993).

Previous studies have revealed that the biocidal activity of Cu(II) is mainly attributed to the cytotoxicity of cellular generated cuprous ion (Cu(I)) (Beswick et al., 1976, Park et al., 2012). Beswick et al. compared the toxicity of Cu(II) and Cu(I) under anoxic conditions; the ED_{50} values of Cu(I) were 10 times lower than those of Cu(II), demonstrating that Cu(I) is more toxic than Cu(II). From the EPR results, they presented direct evidence that a considerable proportion of Cu(II) partially converted to Cu(I), which is a non-paramagnetic species, by the reaction with *E. coli* cells. Park et al. suggested that the microbial effect of Cu(II) mainly resulted from the reaction between copper species and cell components, the penetrated Cu(II) attributed to the cytotoxicity generated Cu(I) intracellularly resulting disruption of cytoplasm.

However, it also has been suggested that Cu(II) can induce oxidative stress by accelerating the production of reactive oxygen species (ROS) during the respiration of bacterial cells, which partially contributes to the lethal action of Cu(II) (Kimura and Nishioka, 1997, Stohs and Bagchi,

1995). Cu(II) mostly functioned as an inducer of the increase of intracellular superoxide levels, causing damage to DNA by the reaction with superoxide-sensitive enzymes.

1.2.2. Copper-based system

As one of the most promising AOPs, the Fenton system produces oxidants such as hydroxyl radical ($^{\bullet}OH$), generated via the decomposition of H_2O_2, and catalyzed by transition metal ions (Fe or Cu). In general, the Fenton reaction can be described as Reaction 1 (M = Fe(II) or Cu(I)).

$$M^{n+} + H_2O_2 \rightarrow M^{(n+1)+} + OH^- + {}^{\bullet}OH \qquad (1)$$

The iron-catalyzed Fenton (-like) systems, the Fe(II)/H_2O_2 and the Fe(III)/H_2O_2 systems (Reaction 2 and 3), are used usually under acidic pH conditions (< pH 3) that require strong acids and bases before and after the processes. While the Fe(II)/H_2O_2 system produces large amounts of waste with fast reaction rate (Reaction 2, k = 63 M^{-1} s^{-1}) (Walling and Goosen, 1973), low concentration of Fe(III)/H_2O_2 can be used, although the rate of reaction is relatively slow (Reaction 3, k = 10^{-3} M^{-1} s^{-1}) (De Laat and Gallard, 1999).

$$Fe(II) + H_2O_2 \rightarrow Fe(III) + OH^- + {}^{\bullet}OH \qquad (2)$$

$$Fe(III) + H_2O_2 \rightarrow Fe(II) + HO_2^{\bullet} + H^+ \qquad (3)$$

With increasing pH, the main oxidant of the Fenton reaction turns to the dominant alternative oxidant, Fe(IV) (Reaction 4).

$$Fe(II) + H_2O_2 \rightarrow Fe(IV) + H_2O \qquad (4)$$

The production of Fe(IV) has been controversial, but it is believed to be less reactive than $^{\bullet}OH$ and has different forms such as oxo- and hydroxo-complexes (Lee et al., 2013, Bataineh et al., 2012, Bernasconi and Baerends, 2009). Previously, researchers have concluded that $^{\bullet}OH$ and Fe(IV) are mainly responsible for the oxidation of organic compounds (Keenan and Sedlak, 2008), and they also inactivate the pathogenic microorganisms (Kim et al., 2010a, Nieto-Juarez et al., 2010).

Copper exhibits a similar reaction mechanism to the Fenton-like chemistry and produces $^{\bullet}OH$ and Cu(III) (Reaction 5 and 6).

$$Cu(II) + H_2O_2 \rightarrow Cu(I) + O_2^{\bullet-} + H^+ \qquad (5)$$

$$Cu(I) + H_2O_2 \rightarrow Cu(II) + {}^{\bullet}OH + OH^- \quad \text{or} \quad Cu(III) + 2H_2O \qquad (6)$$

Recently, a copper-catalyzed Fenton-like system was examined to inactivate the bacteria and viruses (Nguyen et al., 2013, Kim et al., 2015). The Cu(II)/H_2O_2 system showed higher efficiency to MS2 coliphage than *E. coli*, with relatively lower concentrations of approximately 1/100 times. The addition of radical scavenger (t-BuOH) did not affect the MS2 coliphage inactivation, which confirms that the Cu(III) is responsible, rather than $^{\bullet}OH$.

The Fenton (-like) system typically generates highly reactive oxidant, but faces several limitations. pH is an important factor. It is effective only at low pH and the efficiency dramatically decreased due to the speciation change and precipitation. Nevertheless, at neutral pH, different kinds of reactive oxidants, Fe(IV) or Cu(III), are produced, but the H_2O_2 utilization efficiency is accelerated where the oxidant yield is decreased. To overcome the limitations of the Fenton reagent, persulfates, peroxymonosulfate (PMS) or peroxydisulfate (PDS), are adopted as a peroxide that produces hydroxyl radical or sulfate radical.

PMS is decomposed by catalytic reaction via one-electron transfer from the transition metal ion. Transition metals such as Co(II), Fe(II), Ru(III), Ti(III), Ce (III), Mn(II), and Ni(II), mainly produce $SO_4^{\bullet-}$ (Reaction 7) (E^0 ($SO_4^{\bullet-}/SO_4^{2-}$) = + 2.43 V_{NHE}) (Anipsitakis and Dionysiou, 2004, Lente et al., 2009, Zhang and Edwards, 1992, Gilbert and Stell, 1990, Anipsitakis and Dionysiou, 2003, Huie et al., 1991)

$$M^{n+} + HSO_5^- \rightarrow M^{(n+1)+} + SO_4^{\bullet-} + OH^- \qquad (7)$$

$$HSO_5^- + e^- \rightarrow SO_4^{\bullet-} + OH^- \qquad (8)$$

$$HSO_5^- + e^- \rightarrow SO_4^{2-} + {}^{\bullet}OH \qquad (9)$$

The Co(II)/PMS system showed very high efficiencies for the degradation of the contaminants at a much wider pH range (pH 2–8) (Anipsitakis and Dionysiou, 2003, Anipsitakis and Dionysiou, 2004, Anipsitakis et al., 2008). However, few studies have tested the microbial effects of PMS itself or activated PMS systems in combination with activators. Anipsitakis et al. reported the biocidal effect of PMS in combination with cobalt on *E. coli* in pool water, and the efficacy was 4log (99.99%) within 1h using relatively low doses of reagents, 25 ppm of PMS (as Oxone) and 0.1 ppm of cobalt.

1.2.3. Copper-based nanoparticles

With the development of nanotechnology and its applications, the contribution of its noticeable development of and implications for water treatment is receiving attention (Li et al., 2008, Hossain et al., 2014). Nanoparticles (NPs) exhibit antibacterial properties, but the mechanism is not fully understood. Some proposed antimicrobial mechanisms are related to the physical structure of the nanoparticles by damaging the surface of microorganisms, so the size, shape and surface charge of nanoparticles are important. Also, the released metal ions from nanoparticle surfaces may enhances the antimicrobial effect of nanoparticles by penetration to the inside of microorganisms. Table 1.1 summarizes of select studies on nanoparticles that have antimicrobial effects (Seil and Webster, 2012).

Antimicrobial metallic compounds and nanoparticulates such as silver, zinc, magnesium, iron, copper and its oxides or alloys, have been widely studied due to their safety and efficiency against infectious microorganisms. Ag is known as a strong antibiotic and has been widely used; the mechanisms of bacteria inactivation are induced by enzymatic activity, generally reacting with the thiol group of proteins. Both nAg (Sondi and Salopek-Sondi, 2004, Yoon et al., 2007) and Ag^{+} ions (Feng et al., 2000) are effective for gram-positive and gram-negative bacteria. ZnO and MgO exhibited antimicrobial activity at neutral pH, which is a useful property for drinking water treatment. First, it is possible to penetrate the cell membrane with smaller particle size, and its positively charged surface (Huang et al., 2005, Yamamoto, 2001, Jones et al., 2008). When the NPs accumulate in the membrane and cytoplasm of bacteria, they can cause inactivation or growth inhibition (Jones et al., 2008). These NPs can produce reactive oxygens (ROS), such as $O_2^{\bullet-}$ or $^{\bullet}OH$, ultimately generating H_2O_2, and so effectively damaging the carbonyl group of peptide bond, eventually leading to the degradation of protein (Shi et al., 2010).

Recently, several studies have reported the antimicrobial activity of iron-based NPs against *E. coli* (Auffan et al., 2008, Kim et al., 2010b, Lee et al., 2008b) and bacteriophage (You et al., 2005, Kim et al., 2011). nZVI (nano-zero valent iron) inactivated *E. coli* in and absence of oxygen damaging the integrity of the cell membrane and respiratory activity (Lee et al., 2008b, Kim et al., 2010b). Iron-based nanoparticles such as maghemite and magnetite also have been exhibited the cytotoxic effects (Auffan et al., 2008).

Copper nanoparticles (Cu NPs) and copper oxide (CuO) particles are also currently employed with their superior antibacterial activities as silver NPs on various bacteria (Ruparelia et al., 2008, Yoon et al., 2007, Valodkar et al., 2011). For antimicrobial applications, Cu NPs were immobilized on fiber and membrane to treat *E. coli* (Dankovich and Smith, 2014), viruses (Borkow et al., 2007) and fungi (Cioffi et al., 2005). CuO has also been studied, and is known to be relatively less

toxic than copper salt (Bondarenko et al., 2013) showing antimicrobial effects on both Gram-negative and Gram-positive species, *E. coli* and *S. aureus*, respectively. Interestingly, Gram-positive species seemed to be more vulnerable despite the thick cell wall, peptidoglycan layer, such an additional structural barriers (Seil and Webster, 2012).

However, very few papers have addressed the antibacterial activity and toxicity of bimetallic Fe NPs (Marková et al., 2013, Kim et al., 2014). Kim et al. showed the toxicity test on *E. coli* with various additive metal to iron-based NPs, and indicated that oxidative stress and membrane disruption are the major toxicological effect of ambient and engineered NPs.

Table 1.1 Summary of selected studies concerning the antimicrobial effect of nanoparticles

Metal	Size (Average)	Zeta potential	Organism tested	Minimum inhibitory concentrations (MIC)	Proposed mechanism	Ref.
Silver	21 nm	N/A	*E. coli, Vibrio Cholerae, P. aeruginosa*	All reduced 100% at 75 ug/mL	Membrane disruption, Ag ion interference with DNA replication	Morones et al., 2005
Silver	12 nm	Negative (no value)	*E. coli*	Reduced 70% with 10 ug/mL in agar	Membrane disruption, Ag ion interference with DNA replication	Sondi et al., 2004
ZnO	60 nm	N/A	*S. aureus*	Reduced 50% at 400 ug/mL	ROS inhibition	Jones et al., 2008
ZnO	40 nm	Positive (no value)	*S. aureus, E. coli*	Both species reduced 99% at 400 ug/mL	Membrane disruption	Nair et al., 2009
ZnO	12 nm	N/A	*E. coli*	Reduced 90% at 400 ug/mL	Membrane damage due to particle abrasiveness	Padmavathy et al., 2008
ZnO ions	N/A	N/A	*P aeruginosa, S. aureus*	Reduced 100% at 1917, and 9 ug/mL, respectively	ROS inhibition	McCarthy et al., 1992
Cu	100 nm	N/A	*E. coli, B. subtilis*	Reduced 90% at 33.40 ug/mL and 28.20 ug/mL, respectively	Protein inactivation via thiol interaction	Yoon et a., 2007
Fe_3O_4	9 nm	-19.09 mV	*S. Aureus*	Increased dead cells observed at 3 mg/mL	ROS, membrane disruption	Tran et al., 2010
Fe_3O_4	8 nm	N/A	*Staphylococcus epidermidis*	Reduced 65% at 2 mg/mL	ROS, membrane disruption	Taylor et al., 2009
Al_2O_3	11 nm	120 mV	*E. coli*	Reduced 35%, 79% and 68% at 10, 100, and 500 ug/mL, respectively	Dose dependent ROS, particle penetration	Simon-Deckers et al., 2009

Adopted from Seil and Webster, 2012

1.3. Research objectives

Despite the great antimicrobial effects of copper, little is known about the inactivation mechanisms by the copper-based disinfection systems via Fenton-like reaction in neutral pH and natural water. The overall objective of this research was to understand the inactivation of *E. coli* and MS2 coliphage by homogeneous and heterogeneous copper-based disinfection system, and to elucidate the inactivation mechanism that causes the inactivation by these systems at neutral pH.

▶ To investigate the biocidal effects of the combined Cu(II)/HA system on *E. coli* and MS2 coliphage and to gain insight into the mechanism behind the enhanced biocidal actions (Chapter 3)

This study is to assess the biocidal effects of the combined Cu(II)/HA system on *E. coli* and MS2 coliphage and to gain insight into the mechanism behind the enhanced biocidal actions. For these purposes, the inactivation efficacies of *E. coli* and MS2 coliphage by the Cu(II)/HA system are examined at different HA doses, and the effects of dissolved oxygen, copper-chelating agents, and H_2O_2 are investigated. In addition, the level of intracellular oxidants in *E. coli* cells was monitored in response to the addition of Cu(II) and HA. Inactivation experiments were also conducted in natural water samples from surface waters and groundwater to assess the influences of natural organic and inorganic substances.

▶ To investigate possible synergistic effects resulting from the combination of oxidant (i.e. persulfates) with copper ion. (Chapter 4)

This study aimed to investigate possible synergistic effects resulting from the combination of PMS with copper ion. For this purpose, a series of inactivation experiments using surrogate of bacteria, *E. coli*, were carried out in natural water, by varying the concentration of PMS. In addition, to investigate the reactive oxidant produced by the Cu(II)/PMS system, the effects of the scavengers, MeOH, t-BuOH, EDTA and DMP were examined, and the levels of extra- and intracellular oxidants in *E. coli* cells were monitored. Moreover, the inactivation efficacy of the Cu(II)/PMS system on MS2 coliphage was compared with that of *E. coli*.

▶ To evaluate the biocidal effects of iron-based bimetallic nanoparticles (nFeCu) and to gain insight into the mechanism of the enhancement of biocidal effects. (Chapter 5)

For these objectives, the bimetallic nanoparticles were synthesized with iron and copper that are cost effective compared to rare metals such as silver, and to reduce the limitation of nZVI caused by corrosion. Furthermore, this study evaluated the biocidal effects of iron-based bimetallic nanoparticles, nFeCu, to gain insight into the mechanism of the enhancement of biocidal effects, and of the production of biocidal agents. For these purposes, the inactivation efficiency of nFeCu on *E. coli* and MS2 coliphage were examined under various conditions, and the effects of dissolved oxygen, radical scavenger, and copper-chelating reagents were examined. To understand the mechanism of production of reactive oxidants, the role of hydrogen peroxide was evaluated by comparison with nFeCu and the H_2O_2-added to nCu system. Damage of the produced reactive oxidants to *E. coli* and MS2 coliphage was evaluated by microscopic observation after staining by *Bac*Light Live/Dead kit, enzyme-linked immunosorbent assay (ELISA) and the measurement of protein carbonyl group.

Chapter 2. Materials and methods

2.1. Reagents

All chemicals were of reagent grade, and were used without further purification. Agar, nutrient broth, tryptone, yeast extract for *E. coli* and MS2 coliphage cultivation were purchased from Becton-Dickinson Co. (USA). Copper sulfate ($CuSO_4$), hydroxylamine (NH_2OH), Potassium peroxomonosulfate (PMS), hydrogen peroxide (H_2O_2), sodium borohydride ($NaBH_4$), 1,4-piperazinediethanesulfonic acid (PIPES), ethylenediaminetetraacetic acid (EDTA), and 2,9-dimethyl-1,10-phenanthroline (DMP), methanol, *tert*-butanol were used for the inactivation experiments (Sigma-Aldrich Co., USA), and 3′-(p-hydroxyphenyl) fluorescein (HPF) and hydroethidine (HE) for the intracellular oxidant measurements (Invitrogen Co., USA). All solutions were prepared using deionized water (> 18 MΩ·cm, Millipore Co., USA). All glassware was washed with deionized water, and sterilized by autoclave at 121 ℃ for 15 min prior to use.

2.2. Synthesis and characterization of nanoparticles

nFe was synthesized by aqueous-phase reduction of $FeSO_4 \cdot 7H_2O$ adding $NaBH_4$ solution, as described elsewhere (Li et al., 2006, Lee et al., 2008b). $FeSO_4 \cdot 7H_2O$ solution (1.0 g in 200 mL) in deionized water was reduced by the dropwise addition of $NaBH_4$ solution (0.2 g in 50 mL). The suspension of nZVI was washed with acetone 3 times and dried in N_2 chamber overnight. For bimetallic Fe nanoparticles were synthesized by a method similar to the nFe synthesis, followed by displacement plating with $CuSO_4$. After the synthesis of nFe, sodium citrate ($HOC(COONa)(CH_2COONa)_2 \cdot 2H_2O$) was added to the nFe suspension as a stabilizer, then $CuSO_4$ was added and vigorously mixed for 30 min. Collected nanoparticles were washed with 30 mL of acetone for 3 times and dried in N_2 chamber, to prevent surface oxidation (Woo et al., 2014). nCu was prepared as nFe synthesis using $CuSO_4$ solution (0.5 g in 200 mL).

The synthesized materials were characterized using HR-TEM, EDX, XRD, XPS, and BET surface analyzer. The morphologies and sizes and EDX analysis of nanomaterials were performed using JEM-2100F (JEOL). The phase and the crystal structural properties of the nFeCu were determined by XRD (D/Max-2500V/PC, Rigaku) analysis conducted with Cu Kα. The surface

chemistry of the materials was studied using X-ray photoelectron spectroscopy (XPS, K-alpha, ThermoFisher).

2.3. Culture and analysis of microorganisms

E. coli (ATCC 8739) was chosen as a surrogate microorganism for the bactericidal activity test. *E. coli* stock was incubated in 30 mL of Difco nutrient broth at 37 °C for 18–24 h. The cells were harvested by centrifugation at 3000 g for 15 min, and the retained nutrients were removed by washing 3 times with phosphate-buffer saline (PBS, pH 7.2). The obtained *E. coli* cells were resuspended in 20 mL PBS and kept in the refrigerator at 4–5 °C (Nguyen et al., 2013). The spread plate method (Eaton et al., 2005) was employed to determine the population of *E. coli*: the cells plated on nutrient agar were incubated for 24 h at 37 °C, and the number of colonies were counted.

For the virucidal activity test, MS2 coliphage (ATCC 15597-B1) was used with *E. coli* C3000 (ATCC 15597) as a host. The *E. coli* host was cultivated in a growth broth containing 1% tryptone, 0.8% NaCl, 0.1% yeast extract, 0.01% glucose, 2 mM $CaCl_2$ and 0.001% thiamine. MS2 coliphage was incubated in the prepared *E. coli* host for 18–24 h at 37 °C. Subsequently, the cultural solution was centrifuged at 3000 g for 15 min, and the supernatant was filtered with a 0.22 μm PTFE syringe filter (Nguyen et al., 2013). The population of MS2 coliphage was determined by the plaque assay method (Eaton et al., 2005) using a medium of top and bottom double agar layers (0.5 and 1.5% agar, respectively). Further purification for experiments that measured antigenicity or oxidized protein carbonyl group was conducted by filtering the cultured MS2 coliphage by microfiltration (10,000 MWCO, collecting filtrate) and ultrafiltration (20,000 MWCO, collecting retentate) (Cho et al., 2010).

2.4. Microbial inactivation experiments

All experiments were conducted in 60 mL Pyrex flasks at ambient temperature (24 ± 1 °C) under vigorous stirring. A buffered solution of 1 mM PIPES (pH 7.0) was used, except for the experiments using natural waters (unbuffered) or pH-adjusted deionized water. *E. coli* and MS2 coliphage were initially suspended in the buffered solution at approximate populations of 10^7 CFU/mL (or PFU/mL). The inactivation was initiated by simultaneously adding aliquots of reagent stock solutions to the microorganism suspension, or adding the nano materials under vigorous mixing. At pre-determined time intervals, 1 mL of sample was withdrawn into a 1.7 mL polypropylene tube

containing EDTA as quenching reagent to instantly quench the reactions of Cu(II) (Park et al., 2012). Other oxidative reagents, such as PMS or H_2O_2 were quenched by sodium thiosulfate. After serial dilution to certain concentrations, 0.1 mL of each sample was assayed on triplicate agar plates followed by counting the number of viable cells or viruses. The inactivation experiments were repeated more than three times, and the average values and the standard deviations were presented.

For experiments needing deaeration (anoxic conditions), the reaction solution was purged using ultrapure N_2 gas for 30 min prior to the experiment. For some experiments, DMP and EDTA were used as Cu(I)- and Cu(II)-chelating agents, respectively (Patikarnmonthon et al., 2010), and *tert*-butanol and methanol were used as a radical scavenger.

2.5. Natural water samples

Samples were collected from surface water (Chonsang and Hoeya dams in Ulsan city) and groundwater (Jeonbuk Province) sources in South Korea. The waters were filtered through 0.22 μm Nylon membrane filters upon arrival and were stored at 4 °C until use. Several water quality parameters of the samples were analyzed (Table 2.1.).

Table 2.1. Water quality parameters of natural water samples

	pH	Conductivity (μScm^{-1})	Turbidity (NTU)	TOC (mgL^{-1})	A254 (cm^{-1})
Surface water (Hoeya)	7.23	178.10	0.19	2.52	0.05
Surface water (Chunsang)	6.94	123.57	0.13	2.20	0.05
Ground water	7.19	154.8	0.07	0.391	0.00197

2.6. Measurement of intra/extracellular oxidants

The oxidant levels under intracellular and extracellular (free of *E. coli* cells) conditions were determined using cell-permeable fluorescent probe compounds; HPF is for detecting $^{\bullet}OH$ and Cu(III), and HE is for $O_2^{\bullet-}$ (Gomes et al., 2005). *E. coli* cells incorporating probe compounds were used for the measurement of intracellular oxidants. Briefly described, the *E. coli* suspension (10^7 CFU/mL) was mixed with 10 μM of probe compounds for 1 h at 100 rpm in the dark, and washed 2 times with 1 mM PIPES buffer, after centrifugation (5,000 rpm, 5 min). The prepared cells were resuspended in the buffered solution and were treated by different systems using Cu(II) and HA for 30 min. The generated fluorescence intensity was then measured by microplate reader (Infinite M200, Tecan Trading AG, Switzerland). A 485 nm excitation and 535 nm emission filter was used for HPF, and a 535 nm excitation and 590 nm emission filter was used for HE. For extracellular oxidant levels, solutions of HPF or HE without *E. coli* cells were directly used for the fluorescence measurements. The fluorescence intensity ratio (FIR) of each sample, calculated relative to the control containing only the probe compound, was presented. The detailed method for the sample preparation is described elsewhere(Kim et al., 2010b).

2.7. Analyses of Cu(I) and formaldehyde

The concentration of Cu(I) was determined by the neocuproine method(Eaton et al., 2005). The concentration of formaldehyde (HCHO) was measured by DNPH derivatization followed by HPLC analysis with UV absorbance detection at 350 nm. The details are described elsewhere (Keenan and Sedlak, 2008).

2.8. Microscopic analysis by *Bac*Light Live/Dead assay

After *E. coli* suspension treatment by nanomaterials, cells were concentrated by filtering onto 0.2 μm pore-sized black polycarbonate membranes (GE Water & Process Technologies). The *Bac*Light Live/Dead bacterial viability kit (L7012, Molecular Probes) was used to evaluate the membrane integrity. The solution containing SYTO 9 and propidium iodide (PI) was used to distinguish the cells with intact membranes (green fluorescence, live), and with damaged membranes (red fluorescence, dead). 0.3 μL of each component were mixed in 1 mL of deionized water, and the cells were stained with 0.1 mL of staining solution for 1 h in the dark. The number of cells was counted using a 100×oil lens on a microscope (Olympus), with fluorescence for live cells (excitation: 485 nm, emission: 530 nm) and dead cells (excitation: 485 nm, emission: 630 nm) being observed.

2.9. Analysis of antigenicity and oxidized proteins of MS2 coliphage

To analyze the antigenicity of MS2 treated with nFe, nCu and nFeCu, an ELISA assay was performed (MS2 bacteriophage *BioThreat Alert* ELISA kit, Tetracore Inc.). Washing (wash with PBST (PBS with 0.1% Tween-20) for 4 times) and incubation (at 37 °C for 1 h) were conducted before and after the addition of reagents or samples except capture antibody coating step. 100 μL of the capture antibody (rabbit anti-MS2 IgG) diluted to concentration of 2.5 μg/mL in PBS was added to each well of 96-well flat-bottom ELISA plates, incubated overnight at 4 °C and washed with PBST. After coating with capture antibody, each well was blocked with 150 μL of ELISA dilution/blocking buffer (5 g dry skim milk/100 mL PBST) to block all unbound sites. Samples treated by NPs were added, and detector antibody (mouse monoclonal anti-MS2 IgG2a) diluted 2.5 μg/mL in PBST was added to each well. Then the plate was treated by the conjugate antibody (goat anti-mouse IgG-HRP) with 1/5,000 dilution. Finally, ABTS peroxidase substrate was added to the well and the plate was incubated at 37 °C for 30 min in the dark. Absorbance was detected at 405 nm by microplate reader (Infinite M200, Tecan).

The amount of oxidized proteins of MS2 coliphage during the experimental conditions were measured by protein carbonyls using OxiSelect™ Protein Carbonyl ELISA Kit (Cell Biolabs, Inc.) (Cho et al., 2010). The carbonyl groups in the MS2 coliphage and standards were derivatized by DNPH (2,4-dinitrophenylhydrazine) to DNP-hydrazone (2,4-dinitrophenylhydrazone) after incubation at room temperature for 45 min in dark. After the washing steps, blocking buffer and anti-DNP solutions were added to stop the reaction. Subsequently, the samples were incubated with enzyme

substrate, then the absorbance at 450 nm was measured by microplate reader. Detailed experimental procedure was as provided by the manufacturer in the instruction manual.

CHAPTER 3.

Enhanced inactivation of *E. coli* and MS2 coliphage by cupric ion in the presence of hydroxylamine: Dual microbicidal effects

3.1 Results

3.1.1. Enhanced inactivation of *E. coli* and MS2 coliphage by Cu(II) in combination with hydroxylamine

The inactivation of *E. coli* and MS2 coliphage by the Cu(II)/HA system was examined at different input concentrations of HA (Figures 3.1). In control experiments, HA alone had negligible effects on both *E. coli* and MS2 coliphage (data not shown). A Cu(II) concentration of 5 μM resulted 1.5 log inactivation of *E. coli* and less than 0.5 log inactivation of MS2 coliphage in 30 min. The addition of HA significantly enhanced the inactivation efficacies of both *E. coli* and MS2 coliphage. When the concentration of HA was increased, the inactivation rates (calculated from the slopes of inactivation curves in Figures 3.1a and 3.1b) increased by approximately 5–100-fold relative to the conditions with Cu(II) alone; the inactivation rate of MS2 coliphage exhibited a good linearity with the dose of HA.

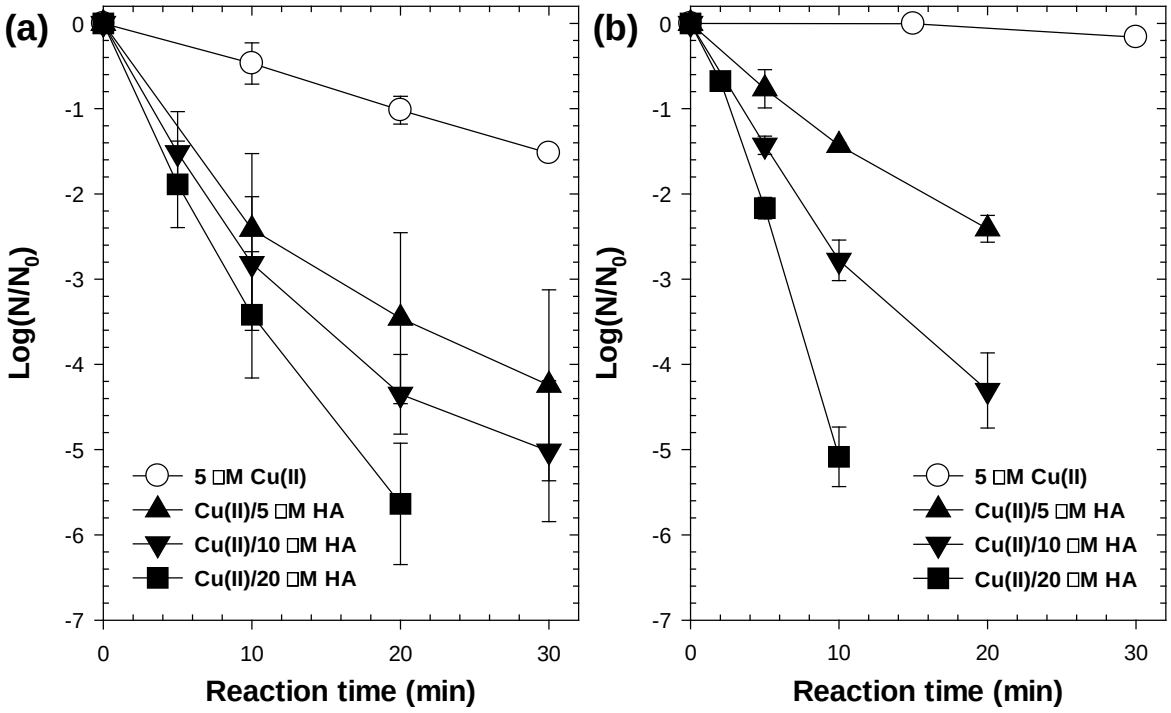

Figure 3.1 Inactivation of (a) *E. coli* and (b) MS2 coliphage by the Cu(II)/HA system as a function of HA concentration. (pH = 7.0, $[Cu(II)]_0$ = 5 μM).

3.1.2. Generation of Cu(I) and reactive oxidants

The generation of Cu(I) by the Cu(II)/HA system was monitored at different HA concentrations under control (oxic) and anoxic conditions (Figure 3.2a). The generation of Cu(I) was enhanced as the concentration of HA increased from 0 to 20 μM under both conditions. However, Cu(I) concentrations were slightly higher overall under anoxic conditions. The production of reactive oxidants by the Cu(II)/HA system was also examined by monitoring the HCHO formation in the presence of excess methanol (Keenan and Sedlak, 2008) (Figure 3.2b). Under oxic conditions, the concentration of HCHO increased with increasing concentration of HA. However, the HCHO formation under anoxic conditions was negligible due to an absence of significant production of reactive oxidants.

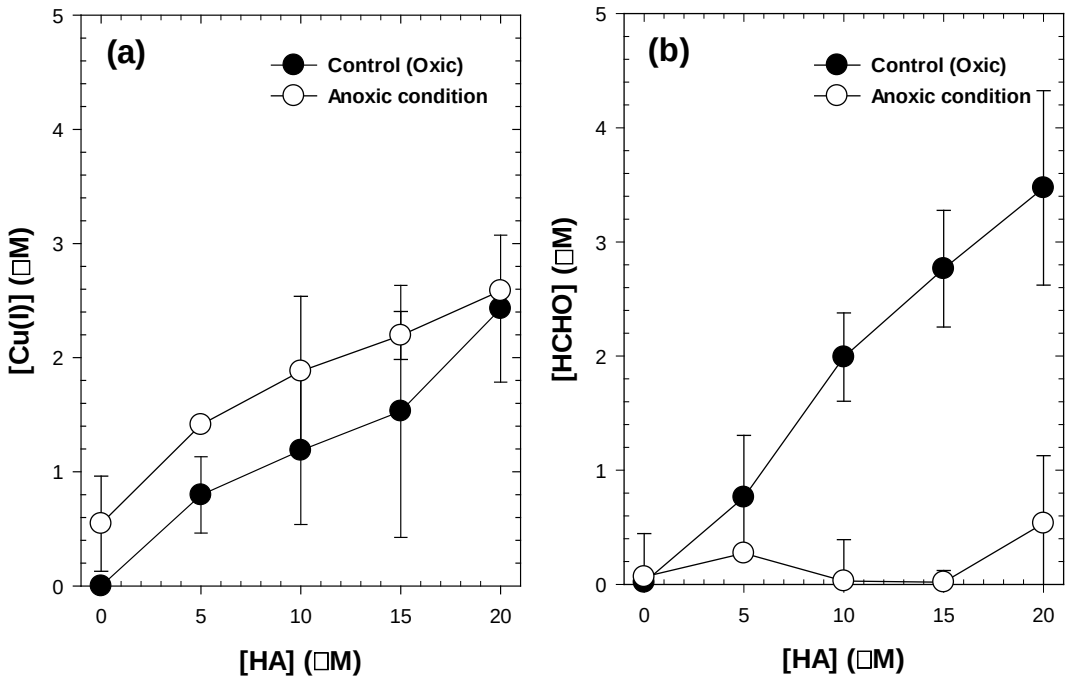

Figure 3.2 (a) Cu(I) generation and (b) HCHO production (from methanol oxidation) by the Cu(II)/HA system. (pH = 7.0, $[Cu(II)]_0$ = 5 μM, reaction time = 30 min, $[Methanol]_0$ = 200 mM for (b)).

3.1.3. Effects of dissolved oxygen, copper-chelating agents, and hydrogen peroxide

The effects of dissolved oxygen, copper-chelating agents (EDTA and DMP), and H_2O_2 on the inactivation of *E. coli* and MS2 coliphage by the Cu(II)/HA system were examined. The time-dependent inactivation curves were obtained under different conditions (refer to Figure 3.3), and the average inactivation rates were presented (Figures 3.4).

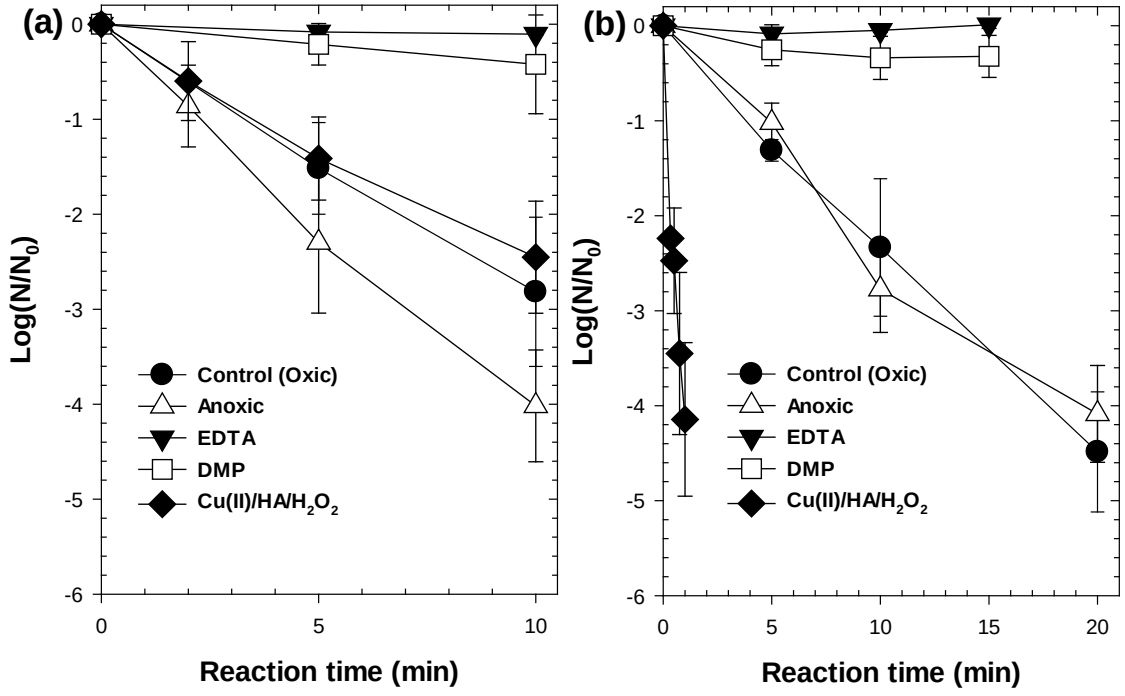

Figure 3.3 Time-dependent inactivation curves. (pH = 7.0, $[Cu(II)]_0$ = 5 μM, $[HA]_0$ = 10 μM, $[EDTA]_0$ = 2 mM, $[DMP]_0$ = 2 mM, $[H_2O_2]_0$ = 10 μM).

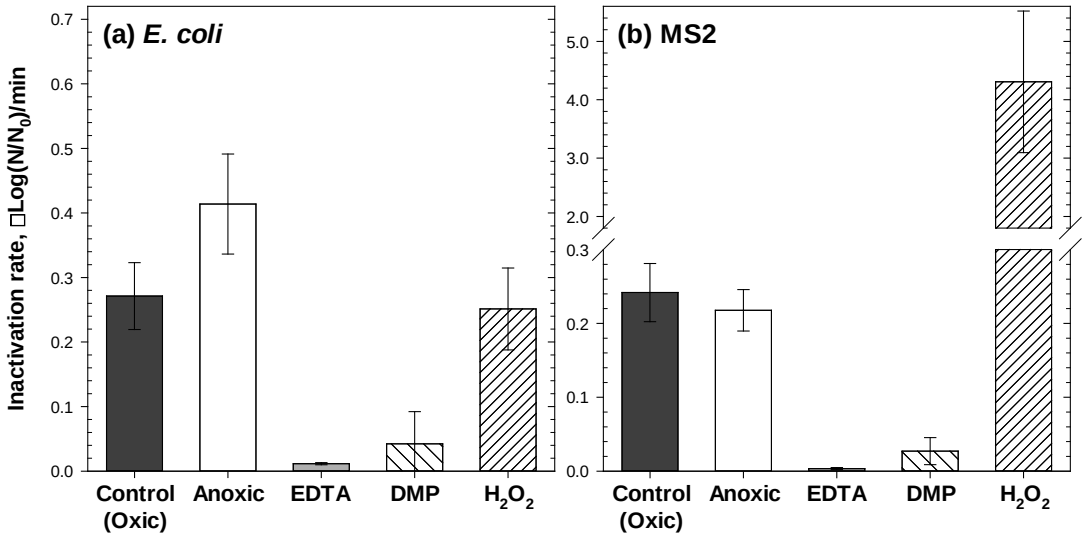

Figure 3.4 Effects of deaeration, copper-chelating reagent, and H_2O_2 on inactivation of (a) *E. coli* and (b) MS2 coliphage by the Cu(II)/HA system. (pH = 7.0, $[Cu(II)]_0$ = 5 μM, $[HA]_0$ = 10 μM, $[EDTA]_0$ = 2 mM, $[DMP]_0$ = 2 mM, $[H_2O_2]_0$ = 10 μM).

The *E. coli* inactivation was significantly enhanced under the anoxic condition compared to the control (Figure 3.4a), whereas the MS2 coliphage inactivation was marginally inhibited under the anoxic condition (Figure 3.4b). The addition of Cu(II)- and Cu(I)-chelating agents (EDTA and DMP) almost blocked the microbial inactivation for both *E. coli* and MS2 coliphage. The addition of 10 μM H_2O_2 did not significantly affect the *E. coli* inactivation by the Cu(II)/HA system (Figure 3.4a). However, the MS2 coliphage inactivation was greatly enhanced by the addition of H_2O_2 (Figure 3.4b); the inactivation rate increased by approximately 20-fold compared to the control.

3.1.4. Generation of Extra/Intracellular Oxidants

Oxidant levels induced by Cu(II), Cu(II)/HA, Cu(II)/H_2O_2, and Cu(II)/HA/H_2O_2 systems (with 0.01 and 1 mM H_2O_2) were determined under extracellular (cell-free) and intracellular (inside *E. coli* cells) conditions for $^{\bullet}OH$ and Cu(III) using HPF (Figure 3.5a) and for $O_2^{\bullet-}$ using HE (Figure 3.5b). The FIR values for $^{\bullet}OH$ and Cu(III) significantly increased only for Cu(II)/H_2O_2 and Cu(II)/HA/H_2O_2 systems with 1 mM H_2O_2 under both extracellular and intracellular conditions

(Figure 3.5a). There were differences in the $O_2^{\bullet-}$ level between the extracellular and intracellular conditions (Figure 3.5b). Under extracellular conditions, the FIR values increased to some degree for most systems; higher FIR values were observed with higher H_2O_2 concentrations for the Cu(II)/H_2O_2 and Cu(II)/HA/H_2O_2 systems. In contrast, the FIR values under intracellular conditions decreased overall.

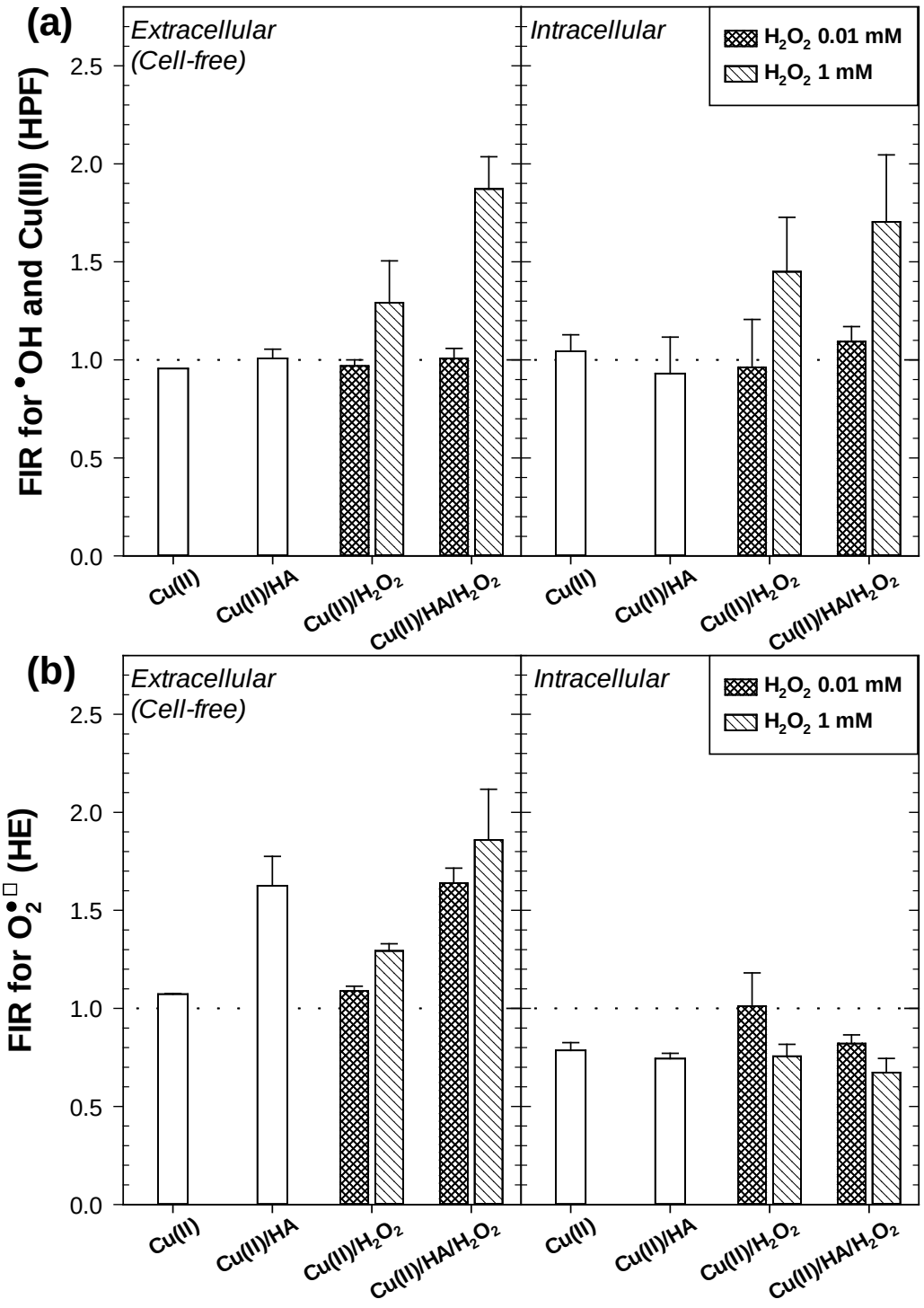

Figure 3.5 Extracellular (cell-free) and intracellular oxidant generation by different Cu(II)-based systems, (a) measurements of $^{\bullet}OH$ and Cu(III) using HPF and (b) $O_2^{\bullet-}$ using HE. (pH = 7.0, $[Cu(II)]_0$ = 5 μM, $[HA]_0$ = 10 μM, $[H_2O_2]_0$ = 10 μM and 1 mM, reaction time = 30 min).

3.1.5. Microbial inactivation in natural waters

The inactivation of *E. coli* and MS2 coliphage by the Cu(II)/HA system was examined in natural waters (Figures 3.6; also refer to Figure 3.7 for the time-dependent inactivation curves). The inactivation of *E. coli* and MS2 coliphage was inhibited in natural waters compared to buffered solution; note that the inhibitory effect was greater for *E. coli* (6–65%) than for MS2 coliphage (17–30%). The inactivation rate of *E. coli* was in the order Buffered water > Surface water (Heoya) > Surface water (Chunsang) > Groundwater, whereas that of MS2 coliphage was in the order Buffered water > Groundwater > Surface water (Heoya) > Surface water (Chunsang).

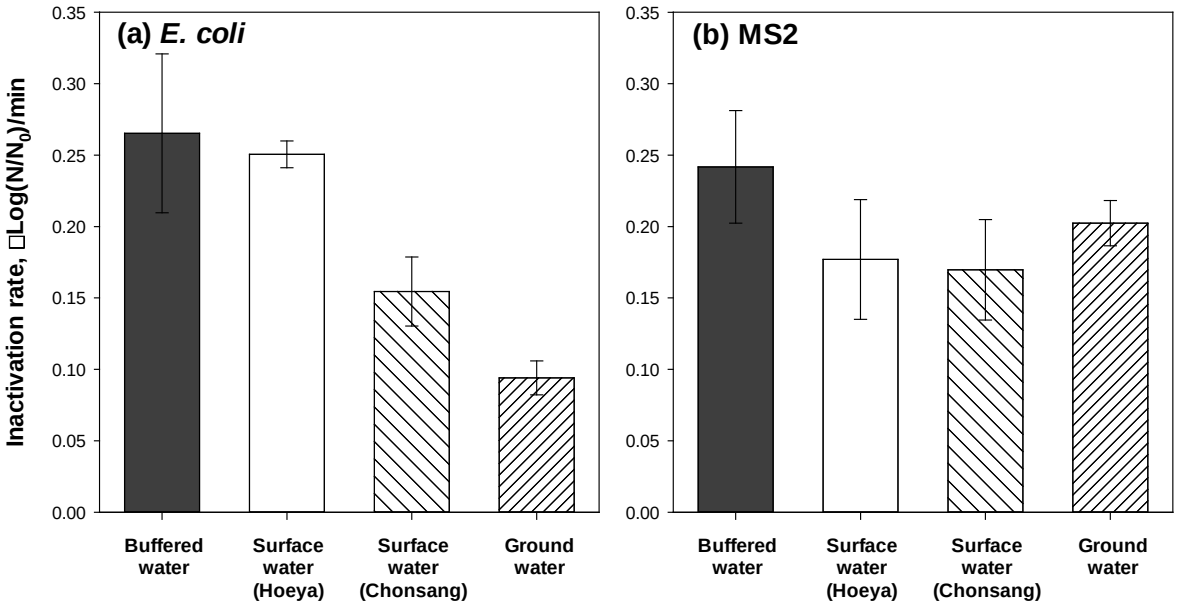

Figure 3.6 Inactivation of (a) *E. coli* and (b) MS2 coliphage by the Cu(II)/HA system in natural waters. (pH = 7.0 for buffered water, $[Cu(II)]_0$ = 5 μM, $[HA]_0$ = 10 μM).

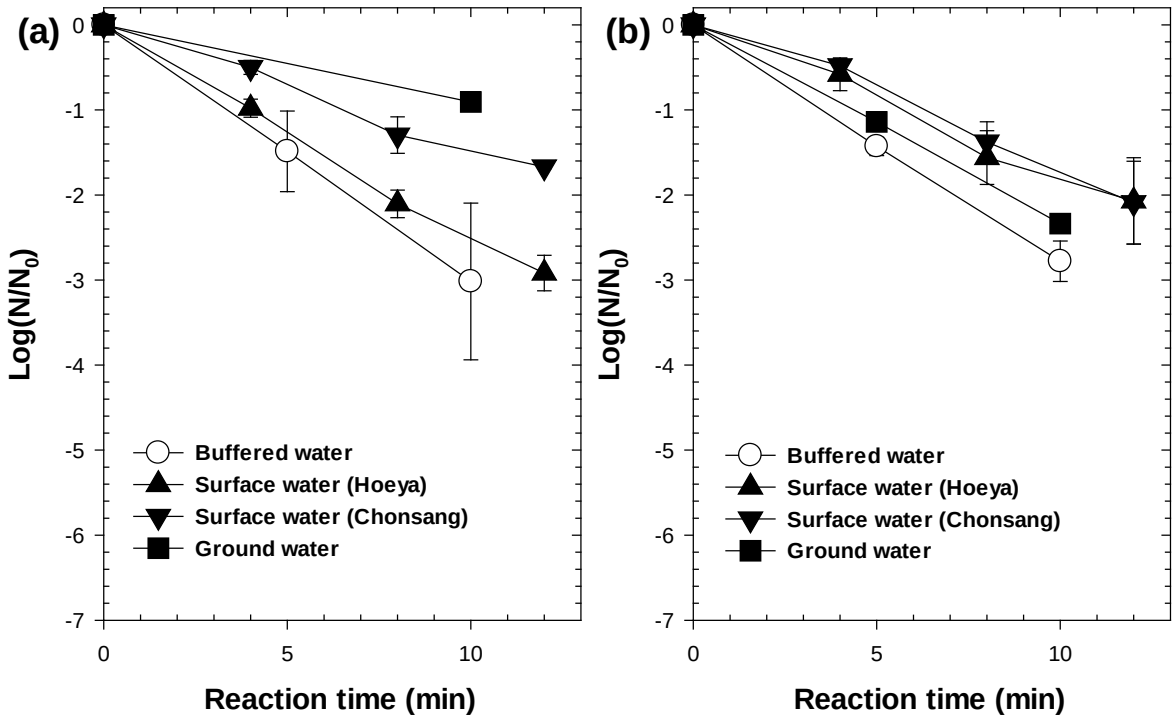

Figure 3.7 Time-dependent inactivation curves for Figure 3.6. (pH = 7.0, $[Cu(II)]_0$ = 5 μM, $[HA]_0$ = 10 μM).

3.2. Discussion

3.2.1. Generation of biocides by the Cu(II)/HA system

Dual biocidal effects (i.e., effects of Cu(I) and reactive oxidants) are anticipated in the Cu(II)/HA system. First, HA as a reducing agent (abiotically) converts Cu(II) into Cu(I) (Reaction 1).(Anderson, 1964) Cu(I) is more cytotoxic and is directly responsible for the biocidal actions of copper compounds. Previous studies have suggested that the bactericidal action of Cu(II) results from the cytotoxicity of Cu(I) that is reductively generated by intracellular cell components(Park et al., 2012, Volentini et al., 2011).

$$2NH_2OH + 4Cu(II) \rightarrow N_2O + H_2O + 4Cu(I) + 4H^+ \quad (1)$$

The enhanced generation of Cu(I) by HA was observed under both oxic and anoxic conditions (Figure 3.2a). Under oxic conditions, concentrations of Cu(I) were lower because dissolved oxygen can oxidize HA as well as Cu(I) (refer to the Reactions below).

Second, the Cu(II)/HA system produces reactive oxidants ($^{\bullet}OH$ or Cu(III)) capable of causing potential oxidative damage to microorganisms by the Fenton-like reaction of the Cu(I) and H_2O_2 generated in situ. The Cu(I) generated by reaction 1 undergoes a series of single-electron transfer reactions in the presence of dissolved oxygen to produce reactive oxidants (Reactions 2−4)(Johnson et al., 1988, Nieto-Juarez et al., 2010, Yuan et al., 2012).

$$Cu(I) + O_2 \rightarrow Cu(II) + O_2^{\bullet-} \quad (2)$$

$$Cu(I) + O_2^{\bullet-} + 2H^+ \rightarrow Cu(II) + H_2O_2 \quad (3)$$

$$Cu(I) + H_2O_2 \rightarrow Cu(II) + {}^{\bullet}OH + OH^- \text{ or } Cu(III) + 2OH^- \quad (4)$$

The reaction of HA with dissolved oxygen can also serve as a source of H_2O_2 for the Fenton-like reaction. In the presence of oxygen, HA is known to be oxidized to N_2 via a two-step process (Reactions 5 and 6) (Tomat et al., 1975) in which H_2O_2 is produced as an intermediate.

$$2NH_2OH + O_2 \rightarrow N_2 + H_2O_2 + 2H_2O \quad (5)$$

$$2NH_2OH + H_2O_2 \rightarrow N_2 + 4H_2O \quad (6)$$

The external supply of H_2O_2 to the Cu(II)/HA system (i.e., the Cu(II)/HA/H_2O_2 system) accelerates the production of reactive oxidants. Indeed, the HCHO formation (from methanol oxidation) was enhanced 2.6-fold by the addition of H_2O_2 (5 μM Cu(II)/10 μM HA vs. 5 μM Cu(II)/10 μM HA/10 μM H_2O_2; data not shown).

According to recent studies(Lee et al., 2014, Nguyen et al., 2013, Pham et al., 2013), Cu(III) (rather than $^{\bullet}OH$) is the dominant oxidant produced by the copper-based Fenton-like reaction (Reaction 4) under neutral pH conditions. Our previous study on the Cu(II)/H_2O_2 system suggested that Cu(III) has strong biocidal activity that is more selective towards a virus surrogate, MS2 coliphage(Nguyen et al., 2013).

Both biocidal effects described above are mediated by the redox reactions of the Cu(II)/Cu(I) couple. EDTA and DMP hinder these redox reactions by forming stable complexes with Cu(II) and Cu(I), consequently eliminating the biocidal activity of the Cu(II)/HA system (Figures 3.4a and 3.4b).

3.2.2. Inactivation of *E. coli*

The enhanced inactivation of *E. coli* by the Cu(II)/HA system is mainly attributed to the biocidal effect of Cu(I) generated by the reduction of Cu(II). This claim is supported by the increased inactivation rate of *E. coli* under anoxic conditions (Figure 3.4a). Compared to oxic condition, the anoxic condition increased the inactivation rate of *E. coli* by 55% (Figure 3.4a), which was consistent with the observation that the Cu(I) concentration increased by 58% (from 1.2 to 1.9 μM) under the same conditions (10 μM HA addition in Figure 3.4a).

It appears that the generation of reactive oxidants by the Cu(II)/HA system does not significantly affect the *E. coli* inactivation, which is supported by multiple observations in this study. First, the HCHO formation (i.e., the indicator for the generation of reactive oxidants) was negligible under the anoxic condition (Figure 3.2b), whereas the *E. coli* inactivation was enhanced. Second, the intracellular oxidant levels in *E. coli* cells did not increase with the Cu(II)/HA treatment. The FIR for $^{\bullet}OH$ and Cu(III) only increased in Cu(II)/H_2O_2 and Cu(II)/HA/H_2O_2 systems with a relatively high dose of H_2O_2 (1 mM) (Figure 3.5a), in which the reactive oxidants may play a role in the *E. coli* inactivation(Nguyen et al., 2013). In addition, the *E. coli* cells treated with the Cu(II)/HA system exhibited different morphologies from those treated with the Cu(II)/H_2O_2 system with high doses of reagents (Figure 3.8). The Cu(II)/HA treatment did not significantly disrupt the integrity of cell membranes (Figure 3.8c).

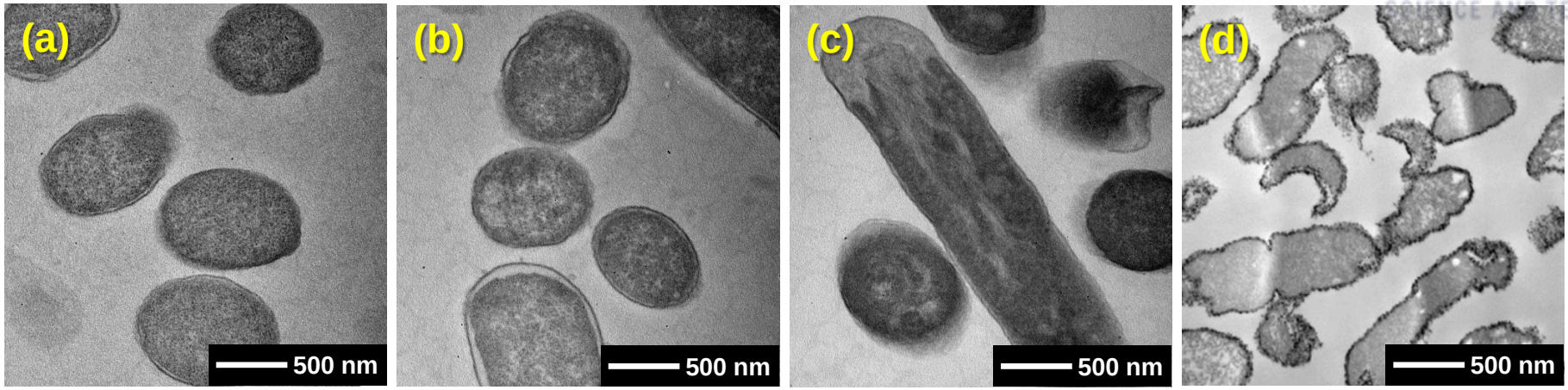

Figure 3.8 TEM images of (a) untreated and treated *E. coli* cells by (b) Cu(II) and (c) Cu(II)/HA. (pH = 7.0, $[Cu(II)]_0$ = 5 µM, $[HA]_0$ = 10 µM, treatment time = 30 min), (d) *E. coli* cells treated by Cu(II)/H_2O_2 ($[Cu(II)]_0$ = 0.1 mM, $[H_2O_2]_0$ = 2.5 mM, treatment time = 30 min) (image from Nguyen et al., 2013).

Method: The morphology of *E. coli* cells before and after the treatment was analyzed using transmission electron microscopy (TEM). The preparation of cells for TEM analysis was performed as described in a previous study(Lee et al., 2008b). The prepared specimens were examined using a JEM-3010 high-resolution electron microscope (Jeol Co., Japan).

Moreover, an interesting observation is that the intracellular $O_2^{\bullet-}$ level decreased for all of the treatment systems (i.e., the FIR values were less than unity), whereas the extracellular $O_2^{\bullet-}$ level in the bulk solution generally increased (Figure 3.5b) (found to cause no lethal damage to the cells[1]). Based on the chemistry of Cu(II) with HA and H_2O_2, there are several routes for the formation of $O_2^{\bullet-}$, which include the oxygen reduction by Cu(I) (Reaction 2) and the oxidation of H_2O_2 by Cu(II) (Reaction 7; particularly important in the Cu(II)/H_2O_2 system) or Cu(III) (Reaction 8).

$$Cu(II) + H_2O_2 \rightarrow Cu(I) + O_2^{\bullet-} + 2H^+ \quad (7)$$

$$Cu(III) + H_2O_2 \rightarrow Cu(II) + O_2^{\bullet-} + 2H^+ \quad (8)$$

These reactions are responsible for the increase in the extracellular $O_2^{\bullet-}$ level; Reaction 2 is responsible for the Cu(II)/HA system, and Reactions 7 and 8 are mainly for the Cu(II)/H_2O_2 and Cu(II)/HA/H_2O_2 systems. However, in the intracellular region, the presence of Cu(II) (which may exist in complexed forms with biomolecules of cell components) appears to favor the consumption of $O_2^{\bullet-}$ regardless of the presence of HA and H_2O_2. The reactions of cell-bound Cu(II) or Cu(III) with $O_2^{\bullet-}$ may be responsible for the $O_2^{\bullet-}$ level drop (Reactions 9 and 10), but further study is needed to clarify the mechanism.

$$\equiv Cu(II) + O_2^{\bullet-} \rightarrow Cu(I) + O_2 \quad (9)$$

$$\equiv Cu(III) + O_2^{\bullet-} \rightarrow Cu(II) + O_2 \quad (10)$$

A similar behavior has been observed in the Cu(II)/H_2O_2 system(Nguyen et al., 2013); the intracellular $O_2^{\bullet-}$ level decreased when increasing the dose of Cu(II).

3.2.3. Inactivation of MS2 coliphage

In contrast with the case of *E. coli*, reactive oxidants (mainly Cu(III)) appear to play a role in the MS2 coliphage inactivation by the Cu(II)/HA system. A slightly higher inactivation rate of MS2 coliphage under the oxic condition compared to anoxic condition supports the involvement of reactive oxidants (Figure 3.4b). In particular, the addition of 10 μM H_2O_2 greatly enhanced the MS2 coliphage inactivation (Figure 3.4b), implying that MS2 coliphage is highly susceptible to the oxidative damage induced by reactive oxidants, which is consistent with previous observations of MS2 coliphage inactivation by the Cu(II)/H_2O_2 system(Nguyen et al., 2013). The addition of 200 mM *tert*-butanol (a

•OH scavenger) did not affect the MS2 coliphage inactivation efficacy in the Cu(II)/HA system (data not shown), confirming that Cu(III) is the responsible oxidant rather than •OH(Nguyen et al., 2013, Lee et al., 2014, Pham et al., 2013).

Despite the role of reactive oxidants, the direct cytotoxicity of Cu(I) cannot be neglected for the MS2 coliphage inactivation by the Cu(II)/HA system. Under the anoxic condition, where reactive oxidants are barely produced (Figure 3.2b), substantial inactivation of MS2 coliphage was observed (Figure 3.4b), indicating that the cytotoxicity of Cu(I) is also important. To sum up, the MS2 coliphage inactivation by the Cu(II)/HA system results from the simultaneous biocidal actions of Cu(I) and reactive oxidants.

CHAPTER 4.

Bactericidal effect of cupric ion combined with peroxomonosulfate in natural water

4.1. Results

4.1.1. Inactivation of *E. coli* by the Cu(II)/PMS system

The inactivation of *E. coli* was examined by the Cu(II), PMS and Cu(II)/PMS system in natural water (Figure 4.1 and 4.2). As control experiments, 0.01 mM of Cu(II) concentration resulted 2-log inactivation in 30 min whereas 0.2 mM of PMS showed negligible effect on *E. coli* inactivation. However, the simultaneous addition of Cu(II) and PMS showed synergistic effect on *E. coli* inactivation, and the inactivation rate increased by approximately 6-fold relative to the condition of the Cu(II) system (Figure 4.1).

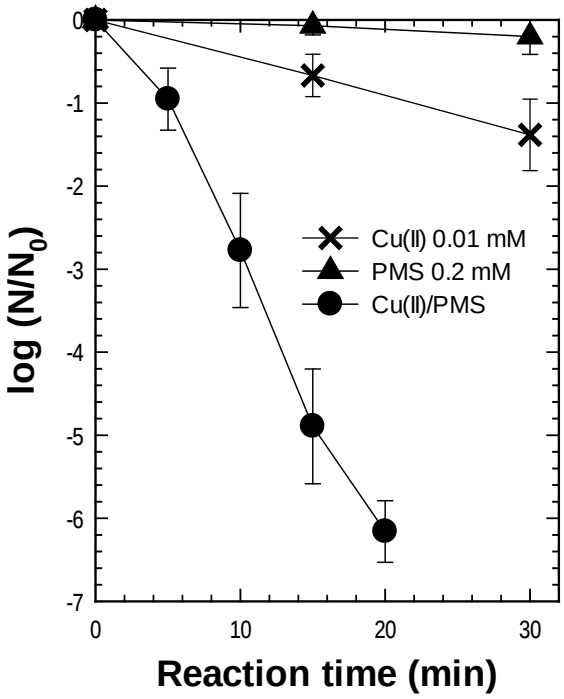

Figure 4.1 Inactivation of *E. coli* by Cu(II) and PMS in natural water. (Natural water from Hoeya DWTP; $[E.\ coli]_0 = 10^7$ CFU/mL; $[Cu(II)]_0 = 0.01$ mM; $[PMS]_0 = 0.2$ mM).

Figure 4.2 demonstrates the effects of the addition of Cu(II) and PMS simultaneously with 0.01 mM of Cu(II) (fixed) and various concentration of PMS. The results were expressed as an inactivation rate, and the inactivation rate divided by time, calculated from the slopes of inactivation kinetics curves. The PMS alone with increase of concentration, from 0.02 to 0.8 mM, did not shown significant efficiency on the inactivation of *E. coli* (Figure 4.2a). However, the inactivation efficiency in the Cu(II)/PMS system was dramatically increased from 5- to 50-fold, compared to the PMS system (Figure 4.2b). As a function of time, the kinetics were alike from 0.2 to 0.8 mM of PMS concentration, but the inactivation efficacy expressed in terms of inactivation rate peaked with 0.4 mM of PMS and partially decreased with further increase of PMS concentration.

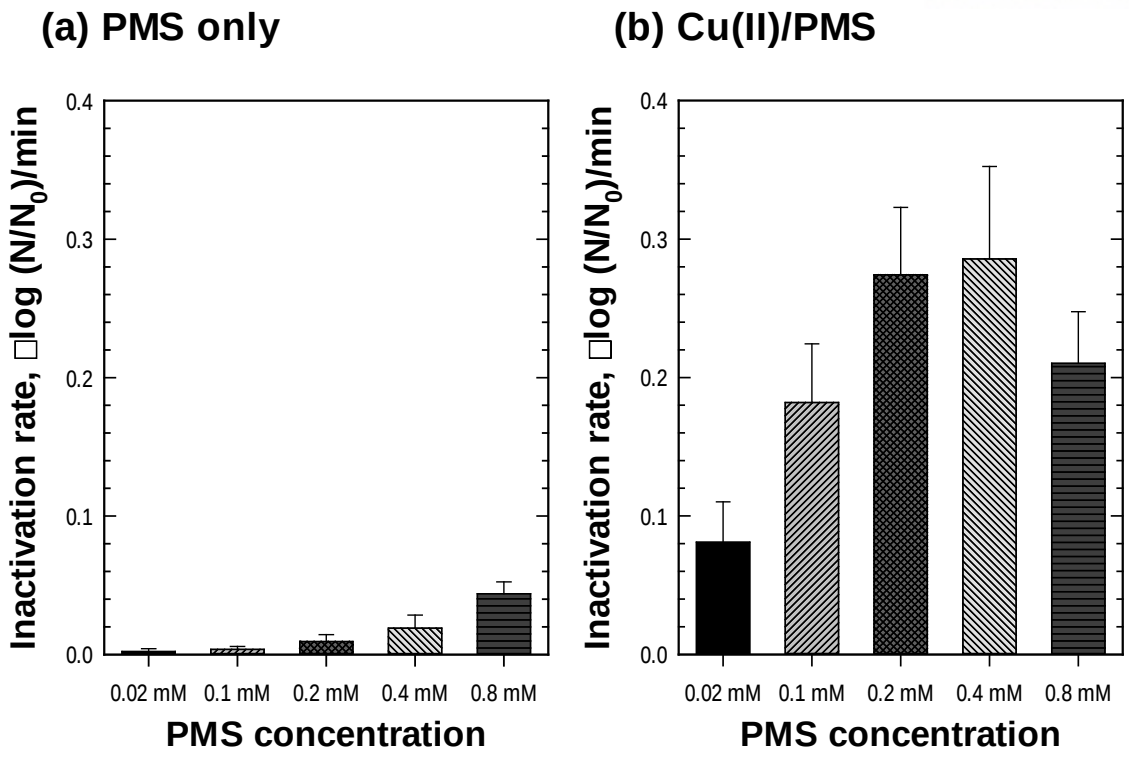

Figure 4.2 Inactivation rate of *E. coli* with Cu(II) and PMS in natural water with various concentration of PMS: (a) PMS only, and (b) Cu(II)/PMS system. (Natural water from Heoya DWTP; $[E.\ coli]_0 = 10^7$ CFU/mL; $[Cu(II)]_0 = 0.01$ mM; $[PMS]_0 = 0.02, 0.1, 0.2, 0.4, 0.8$ mM).

4.1.2. Scavenging effect on the Cu(II)/PMS system

The effects of scavengers, methanol, t-BuOH, EDTA and DMP were examined and the average inactivation rates are presented (Figure 4.3). The concentration of PMS, 0.2 mM, was chosen that showed saturated efficiency in combination with Cu(II). The addition of radical scavengers, MeOH and t-BuOH, marginally inhibited the *E. coli* inactivation, up to 10%, compared to the control. However, the addition of Cu(II)- and Cu(I)-chelating agents (EDTA and DMP) almost blocked the biocidal effect of the Cu(II)/PMS system.

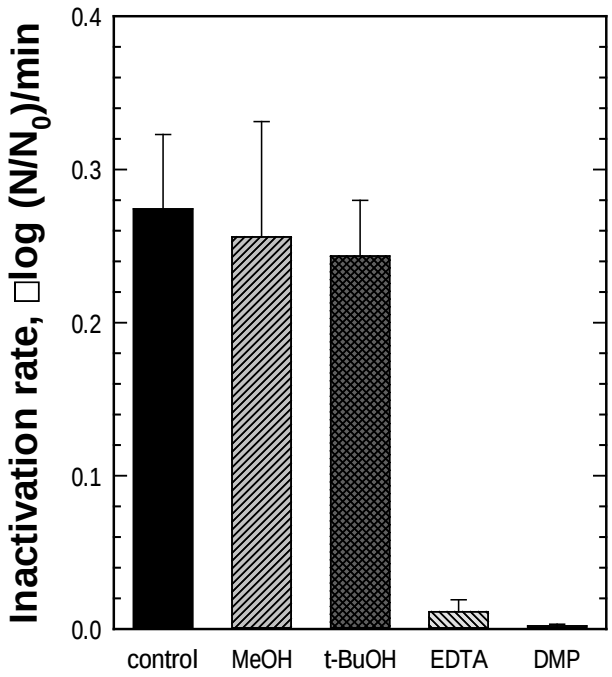

Figure 4.3 Scavenging effect on the inactivation of *E. coli* by the Cu(II)/PMS system. (Natural water from Heoya DWTP; $[E.\ coli]_0 = 10^7$ CFU/mL; $[Cu(II)]_0 = 0.01$ mM; $[PMS]_0 = 0.2$ mM; [MeOH] = [t-BuOH] = 200 mM; [EDTA] = [DMP] = 2 mM).

4.1.3. Effects of the sequential addition of Cu(II) and PMS

To compare the three different systems, Cu(II), PMS, and Cu(II)/PMS system, the sequential treatment were examined to understand how to apply the Cu(II)/PMS system to the real water treatment system more effectively. The sequential addition of the second additive was carried out after 15 minutes of pre-treatment of the first reagent without any further scavenging of the first additive, and finally the inactivation reaction was performed as a combined system (Figure 4.4a, dashed line). The inactivation kinetics of sequential addition was markedly enhanced when both the reagents reacted in combination. In terms of inactivation rate, the sequential addition system of Cu(II) followed by PMS showed the best efficiency of about 3.5-fold that of the combined system. However, the sequential system that of PMS followed by Cu(II) showed only 1.5-fold enhancement (Figure 4.4b).

The results show that damaged cells with Cu(II) in reactor were more vulnerable and could be inactivated by the secondary additive, PMS, as a combined system.

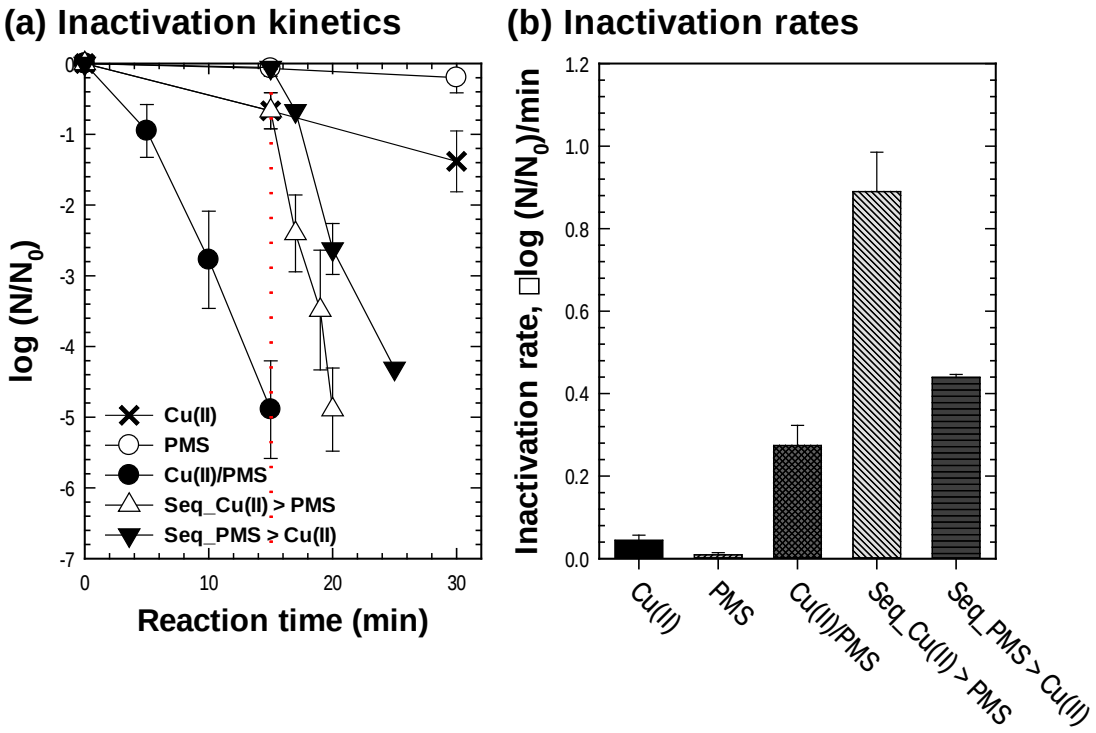

Figure 4.4 Inactivation (a) kinetics and (b) rates of the sequential addition by the Cu(II)/PMS system. (Natural water from Heoya DWTP; $[E.\ coli]_0 = 10^7$ CFU/mL; $[Cu(II)]_0 = 0.01$ mM; $[PMS]_0 = 0.2$ mM; Reaction rates of sequential addition were calculated from 15 min, second additives were added.).

4.1.4. Generation of extra- or intra-cellular oxidants.

The oxidant levels of extra- (cell-free) and intracellular (inside of *E. coli* cells) region were determined by cell-permeable fluorescent probe compound (Figure 4.5); HPF detects highly reactive oxygen species such as hydroxyl radical and reactive intermediates of peroxidase(Ito and Kawanishi, 1991, Gomes et al., 2005). There was not much differences of FIR values under both extra- and intracellular conditions after Cu(II) or PMS treatment, except that the value of the intracellular region treated by the Cu(II) system decreased. However, the Cu(II)/PMS system showed enhancement of the

FIR value under both extra- and intracellular conditions; much higher increase was presented at the intracellular region.

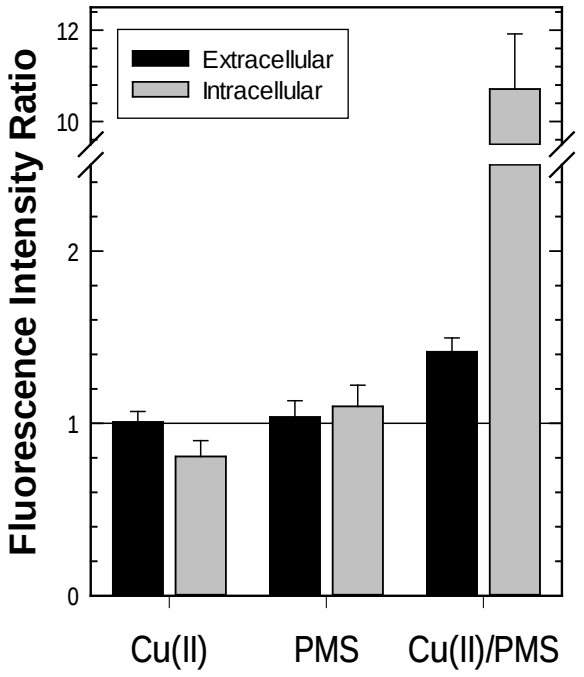

Figure 4.5 ROS generation of the Cu(II)/PMS system. (Natural water from Heoya DWTP; $[E.\ coli]_0 = 10^7$ CFU/mL; $[Cu(II)]_0 = 0.01$ mM; $[PMS]_0 = 0.2$ mM; Reaction time = 30 min).

4.1.5. Inactivation of MS2 coliphage by the Cu(II)/PMS system

The inactivation of MS2 coliphage by Cu(II), PMS and the Cu(II)/PMS system was examined in natural water, and the averaged inactivation rates are presented by the calculation of the slope from the inactivation curves (Figure 4.6). The PMS system showed the inactivation efficiency on MS2 coliphage gradually increased as the PMS concentration increased (Figure 4.6a) as shown in *E. coli* inactivation (Figure 4.2a). The combined Cu(II)/PMS system showed the synergistic effect on MS2 coliphage, but the efficacy was lowered to half that of *E. coli* (Figure 4.6). While the PMS concentration varied from 0.02 to 0.8 mM, the inactivation rate with 0.2 mM of PMS showed the highest value.

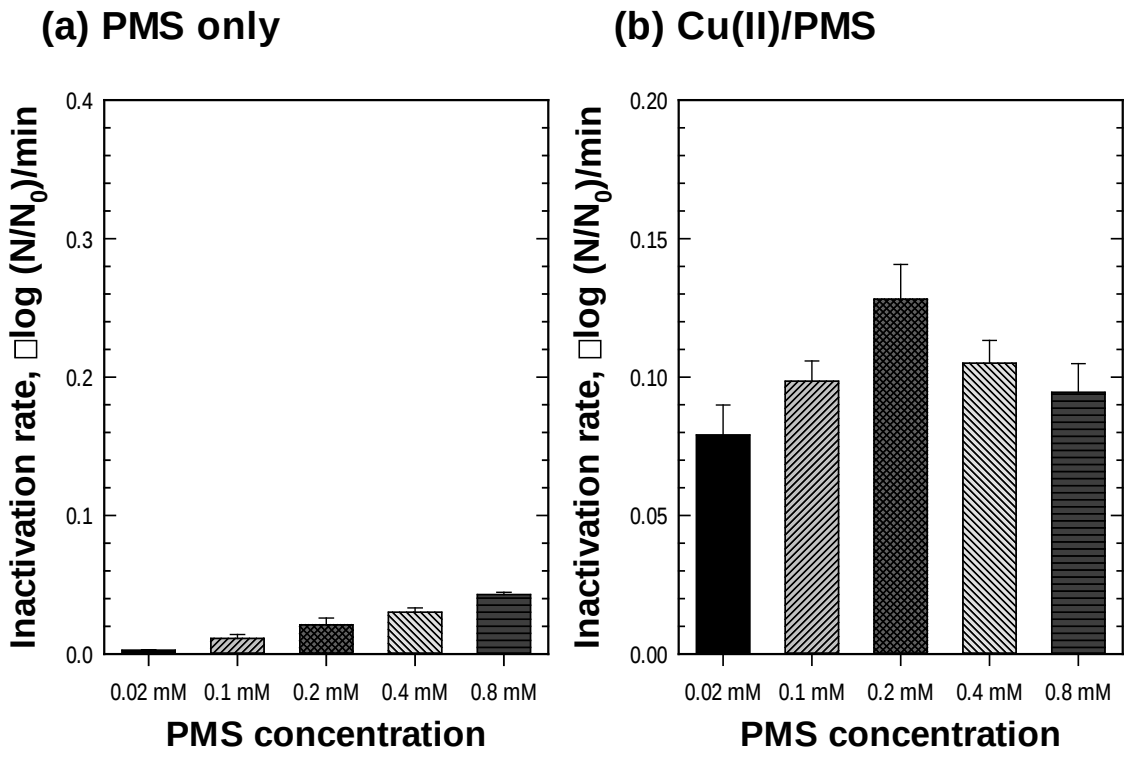

Figure 4.6 Inactivation rate of MS2 coliphage with Cu(II) and PMS in natural water with various concentration of PMS: (a) PMS only, and (b) Cu(II)/PMS system. (Natural water from Heoya DWTP; $[MS2\ coliphage]_0 = 10^7$ PFU/mL; $[Cu(II)]_0 = 0.01$ mM; $[PMS]_0 = 0.02$, 0.1, 0.2, 0.4, 0.8 mM).

4.2. Discussion

4.2.1. Generation of biocides by the Cu(II)/PMS system

The PMS did not show much inactivation effect on either *E. coli* or MS2 coliphage for the tested concentration range, from 0.02 to 0.8 mM (Figure 4.2a, 4.6a). However, it appears that the generation of reactive oxidants by the combined system, the Cu(II)/PMS system, is effective for both bacteria and virus, *E. coli* and MS2 coliphage (Figure 4.2b, 4.6b).

First, transition metals like iron or copper transfer electrons to persulfate, then generate radicals such as sulfate radical ($SO_4^{\bullet-}$) (Reaction 1) or hydroxyl radical ($^{\bullet}OH$) (Reaction 2), in general. The sulfate radicals are known that have greater oxidative potential (E^0 ($SO_4^{\bullet-}/SO_4^{2-}$) = 2.43 V_{NHE}) (Huie et al., 1991) than persulfate and can further generate other reactive species.

$$Cu(II) + HSO_5^- \rightarrow Cu(III) + SO_4^{\bullet-} + OH^- \quad (1)$$

$$H_2O + SO_4^{\bullet-} \rightarrow H^+ + SO_4^{2-} + {}^{\bullet}OH \quad (2)$$

The radical scavengers, MeOH and t-BuOH, were employed to investigate the generated radical species. The hydroxyl radical reaction can be scavenged by MeOH (k = (3.8−7.6) × 10^8 M^{-1} s^{-1}) and t-BuOH (k = 6.0 × 10^8 M^{-1} s^{-1}) (Buxton et al., 1988). The sulfate radical reacts with MeOH (k = 3.2 × 10^6 M^{-1} s^{-1}) and t-BuOH (k = (4−9.1) × 10^5 M^{-1} s^{-1}) (Neta et al., 1988, Anipsitakis and Dionysiou, 2004) much more slowly. However, the scavenging effect of both scavengers, MeOH and t-BuOH, was not significant in the Cu(II)/PMS system, so we conclude the predominant agent would not be the hydroxyl radical. After all, we found that there was a little generation of reactive oxidants detected by the HPF in bulk, in the extracellular region (Figure 4.5).

Second, resulting from injected copper, Cu(II), Cu(III) or Cu(I) can be produced that can possibly cause potential oxidative damage on microorganisms. Cu(III) also has great biocidal activity, and is known to be more selective toward MS2 coliphage (Nguyen et al., 2013). PMS can reduce Cu(II) into Cu(I) via one-electron transfer (Reaction 3) and PMS activation can occur subsequently by Cu(I) (Reaction 4) (Ding et al., 2013).

$$Cu(II) + HSO_5^- \rightarrow Cu(I) + SO_5^{\bullet-} + H^+ \quad (3)$$

$$Cu(I) + HSO_5^- \rightarrow Cu(II) + SO_4^{\bullet-} + OH^- \quad (4)$$

Cu(I) is more likely to inactivate bacteria, by the interaction with thiol groups of cell components, causing the denaturation of proteins (Park et al., 2012, Smith and Reed, 1992).

4.2.2. Role of copper

The Cu(II) plays an important role in the inactivation mechanism of the Cu(II)/PMS system. The effects of Cu(II) were simply identified by the Cu(I)- and Cu(II)-chelating reagent, DMP and EDTA, inhibiting the biocidal effect of the Cu(II)/PMS system (Figure 4.3). Copper is known to

disrupt the enzyme structure and function binding thiol or other groups on protein molecules (Sterritt and Lester, 1980, Smith and Reed, 1992). Not only the effect of copper-induced damage on cells, the bound copper ions on cell surfaces may act as reaction site, confirming that the effect of copper was significant with the sequential addition of Cu(II) followed by PMS (Figure 4.4). The ROS generation fluorescence intensity ratio (FIR) value was enhanced about 11-fold under intracellular condition, whereas the FIR value was only increased 1.5-fold under extracellular conditions, compared to the initial value. It is hard to determine the exact amount of reactive oxidants by the fluorescence intensity, but the ratio can be interpreted to mean that the Cu(II)/PMS system produced relatively higher concentration under intracellular condition. We assume that this resulted from the Cu(I) bound to cells, as stated above, or that accumulated Cu(II) ions can react with PMS to produce reactive oxidants.

CHAPTER 5.

Enhanced microbicidal effects of bimetallic iron-copper nanoparticles

5.1. Results

5.1.1. Characterization of materials

TEM images show bimetallic nFeCu nanoparticles ranging 20–70 nm in diameter, in agreement with previous studies (Li et al., 2006, Lee et al., 2008b), primarily, the nZVI forms chain-shaped aggregations of spherical nanoparticles (Figure 5.1). nFeCu was similar to bare nFe (data not shown), the additive Cu layered onto the nFe structure like core-shell structure or adhered to the surface as particles. Various sites (sites A–E) of the nanoparticles were examined by EDX analysis to further quantify the surface and contents. The surface of NPs was partially oxidized and the oxygen contents by EDX ranged up to about 17%. The contents of iron and copper in nFeCu were measured by AA after dissolving in HNO_3; the ratio of iron to copper was 7.5:1.

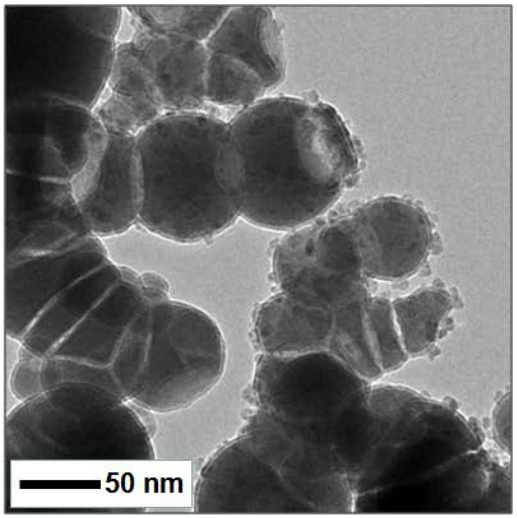

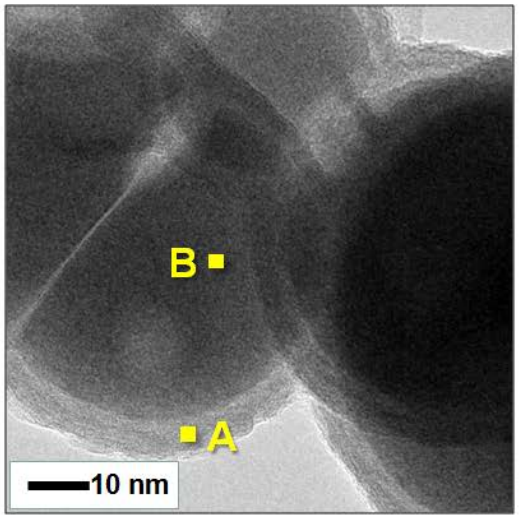

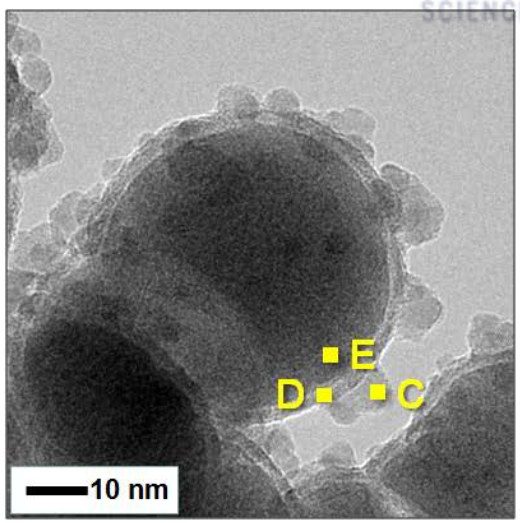

Site A

Element	Wt%
O	20.87
Fe	33.64
Cu	45.49
Total:	100.00

Site B

Element	Wt%
O	6.34
Fe	78.24
Cu	15.42
Total:	100.00

Site C

Element	Wt%
O	5.02
Fe	0.32
Cu	94.66
Total:	100.00

Site D

Element	Wt%
O	16.66
Fe	21.97
Cu	61.37
Total:	100.00

Site E

Element	Wt%
O	5.89
Fe	53.99
Cu	40.12
Total:	100.00

Figure 5.1 TEM and EDS analysis of the nFeCu.

Figure 5.2 shows the XRD and XPS results of synthesized nFeCu. XRD spectrum (Figure 5.2a) shows a broad peak that suggesting an amorphous phage of iron. The most presented peak centered at 2θ of 44.9° indicates the presence of zero-valent iron (α-Fe) (Sun et al., 2006, Wang et al., 2008). However, the peak of copper was not significantly present.

XPS spectra (Figure 5.2b) show the existence of iron and copper with oxide form. The peaks at 710.9 and 724.4 eV suggest that the surface contains a layer of iron oxide, such as Fe_2O_3 or Fe_3O_4, and a clear shoulder at around 706.6 eV implies a $2p_{3/2}$ peak of zero valent iron(Wang et al., 2008). The spectra of CuO and CuO_2 show peaks at 932.5 and 952.eV, respectively, and core-level copper binding energies at 952 eV were reported that coincide with CuO (Midander et al., 2009).

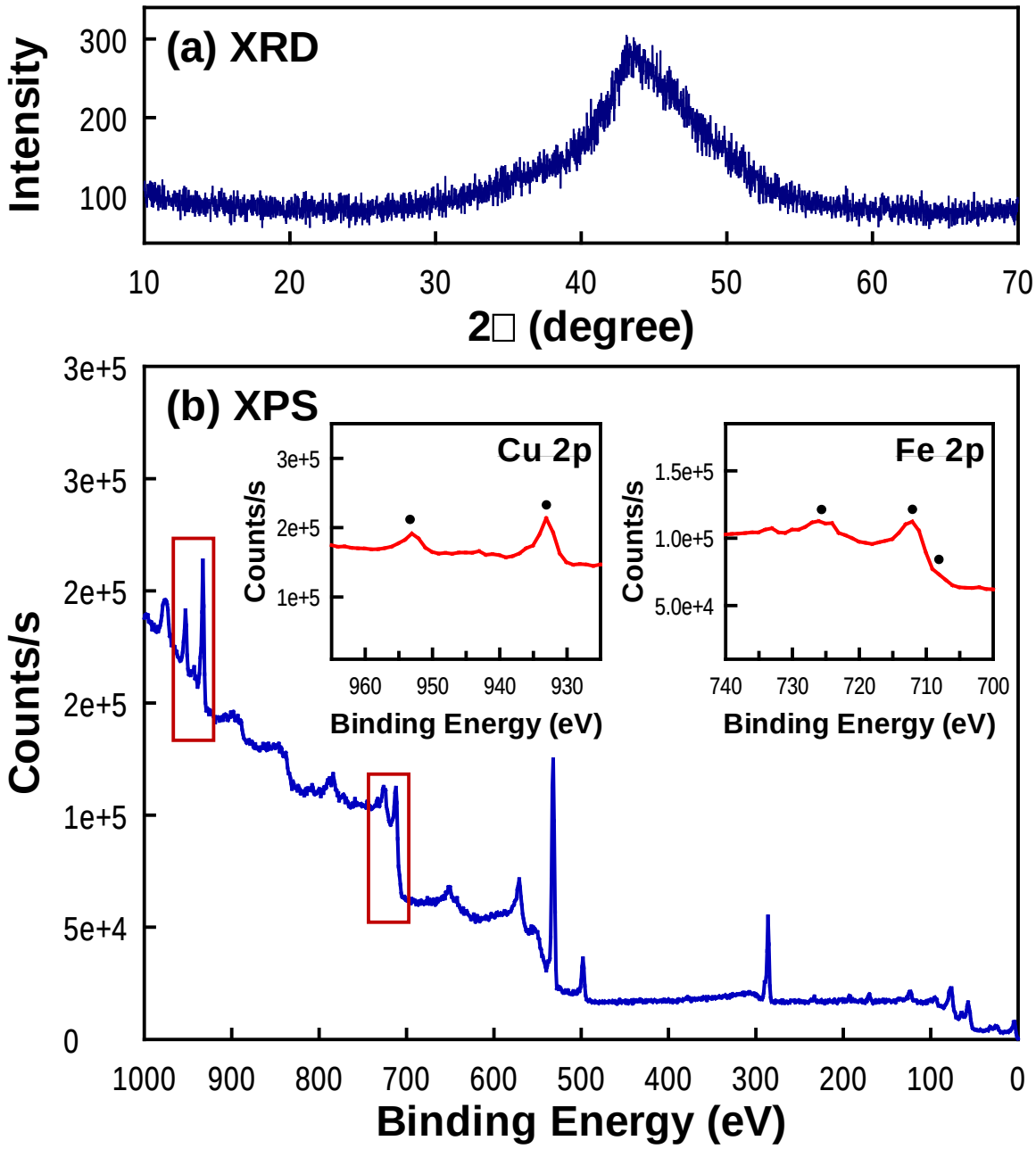

Figure 5.2 (a) XRD patterns and (b) XPS spectra of the nFeCu.

5.1.2. Microbicidal effect of nanomaterials

The inactivation of *E. coli* and MS2 coliphage was examined by the NPs, nFe, nCu and nFeCu (Figure 5.3 and 5.4). Figure 5.3 indicates the inactivation of *E. coli* with NPs ([NPs] = 0.05 g/L) at pH 6 in the presence and absence of oxygen. At the ambient condition, nFe has negligible bactericidal effect on *E. coli*. The inactivation rate of nFeCu increased by approximately 2.5-fold relative to the condition with nCu, resulting in 3log inactivation for 15 min. The inactivation efficiency of nFeCu and nFe was extremely enhanced under anoxic conditions, from 5 to 50 times in terms of inactivation rate, respectively. nCu showed a 1log decrease of the inactivation efficiency compare to the ambient condition.

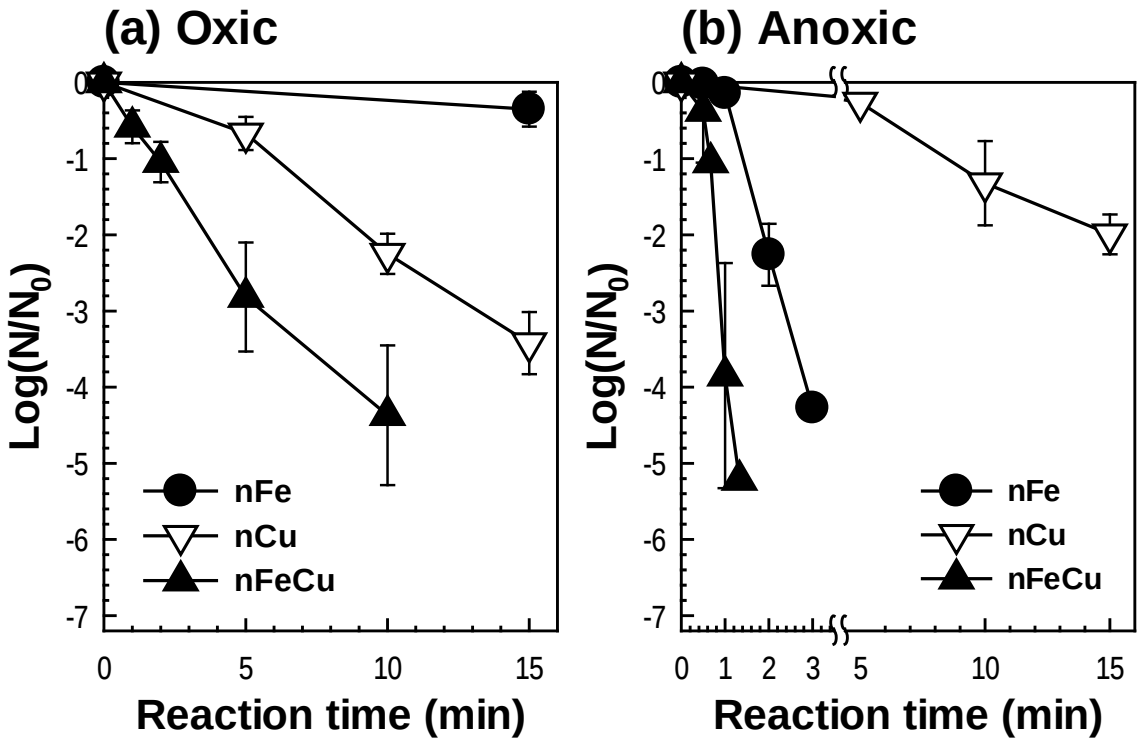

Figure 5.3 Inactivation of *E. coli* by the zero-valent nanomaterials in the (a) presence and (b) absence of oxygen. ([*E. coli*] = 10^7 CFU/mL; [nFe] = [nCu] = [nFeCu] = 0.05 g/L; $pH_{f, avg.}$ = 6.3).

The inactivation of MS2 coliphage was examined with nFe, nCu and nFeCu (Figure 5.4). Under oxic conditions, the virucidal effects of NPs were similar to the bactericidal effects (nFe < nCu < nFeCu). In contrast with the case of *E. coli*, inactivation of MS2 coliphage by NPs significantly decreased under anoxic conditions.

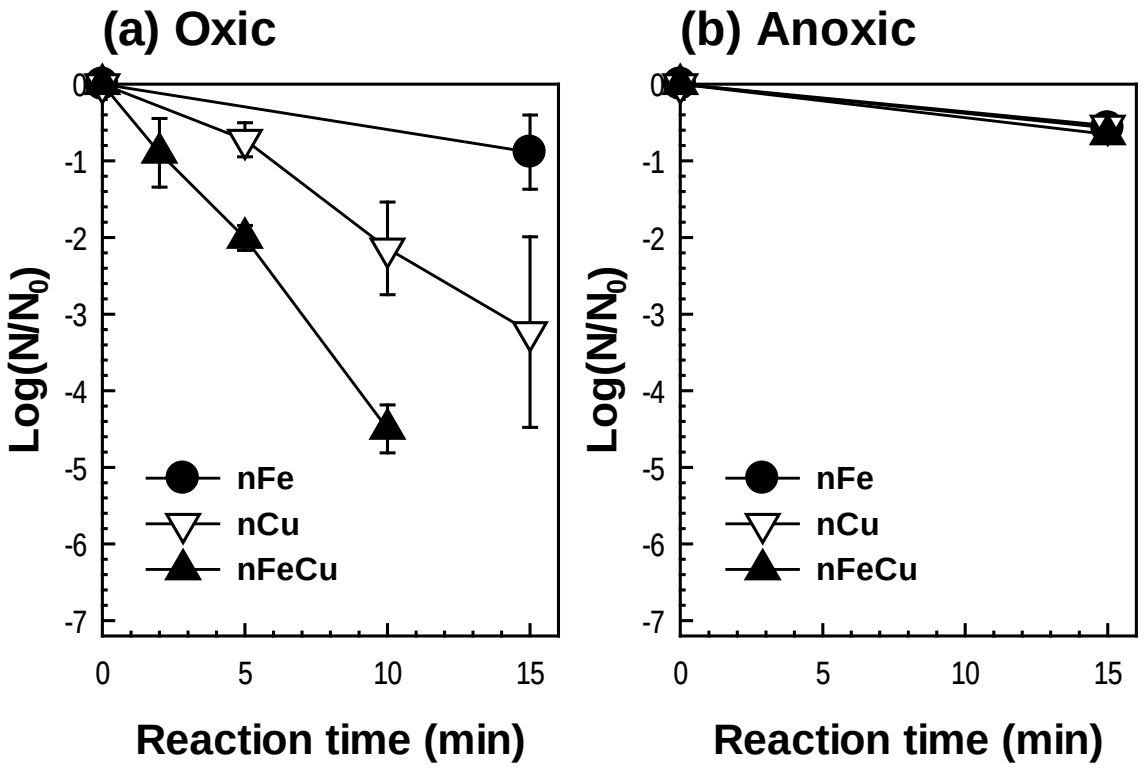

Figure 5.4 Inactivation of MS2 coliphage by the zero-valent nanomaterials in the (a) presence and (b) absence of oxygen. ([MS2 coliphage] = 10^7 PFU/mL; [nFe] = [nCu] = [nFeCu] = 0.05 g/L; $pH_{f,\ avg.}$ = 6.3).

5.1.3. Scavenging effect of methanol and copper-chelating reagent

The effects of methanol and copper-chelating agents (EDTA and DMP) on the inactivation of *E. coli* and MS2 coliphage by the nFeCu were examined and the average inactivation rates are presented (Figure 5.5). The *E. coli* inactivation was marginally inhibited by methanol compared to the control, whereas the MS2 coliphage inactivation was inhibited about 40%, which indicates the effects of reactive oxidants. The addition of Cu(I)-chelating reagent, DMP, partially inhibited both the bactericidal and virucidal effects of nFeCu, 70% and 20%, respectively. Meanwhile the addition of Cu(II)-chelating reagent, EDTA, almost blocked the microbial inactivation effects of nFeCu for both *E. coli* and MS2 coliphage.

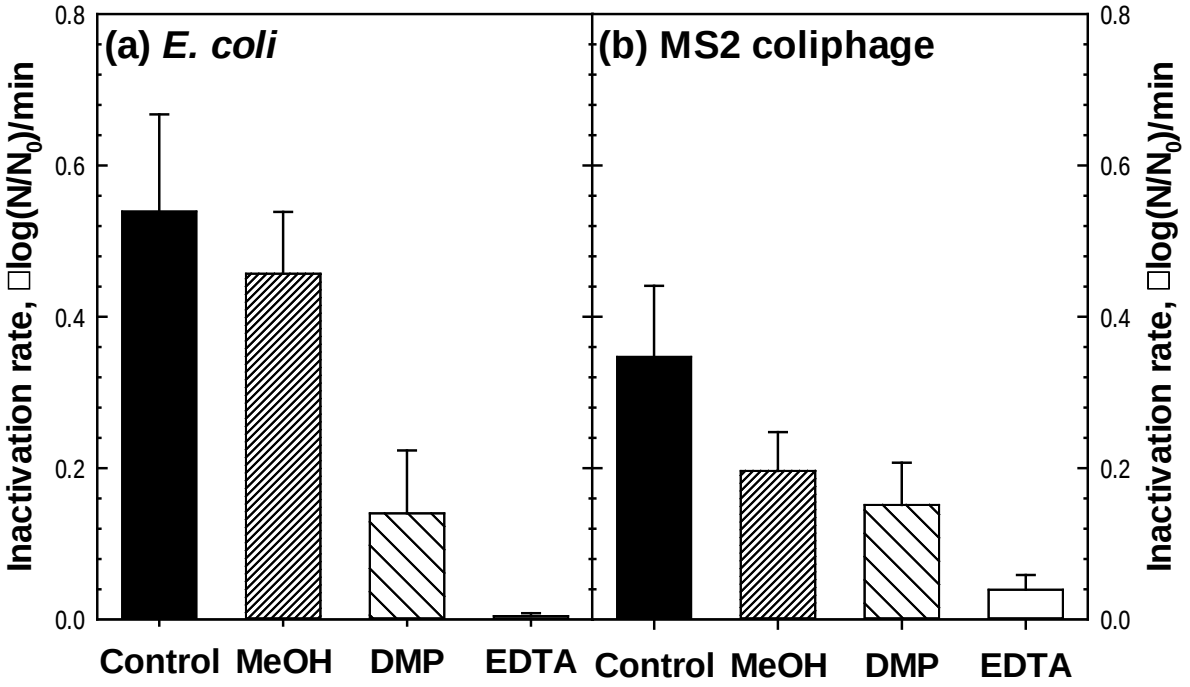

Figure 5.5 Effects of methanol and copper-chelating reagent on the inactivation of (a) *E. coli* and (b) MS2 coliphage by the zero-valent nanomaterials. ([*E. coli*] = 10^7 CFU/mL; [MS2 coliphage] = 10^7 PFU/mL; [nFeCu] = 0.05 g/L; $pH_{f, avg.}$ = 6.3; [MeOH] = 10 mM; [DMP] = [EDTA] = 2 mM).

5.1.4. ROS generation

The generated oxidant levels by NPs and the nCu/H_2O_2 system were examined by varying the concentration of H_2O_2 under intracellular conditions (inside of the *E. coli* cells) and extracellular conditions (bulk solution) (Figure 5.6). nZVI is known to produce H_2O_2 in the presence of oxygen during the corrosion process of nZVI in situ (Joo et al., 2004, Joo et al., 2005). The addition of H_2O_2 to the nCu system was tested to evaluate the production of the reactive oxidants. Under both extracellular and intracellular conditions, nFe showed the highest fluorescence intensity ratio (FIR) for HPF followed by nFeCu and nCu. The addition of H_2O_2 with various concentrations to nCu had no effect on the generation of oxidant in bulk solution. Under the intracellular condition, the addition of H_2O_2 to the nCu showed increase of FIR compared to the nCu only system, but the variation of H_2O_2 concentration had no correlation.

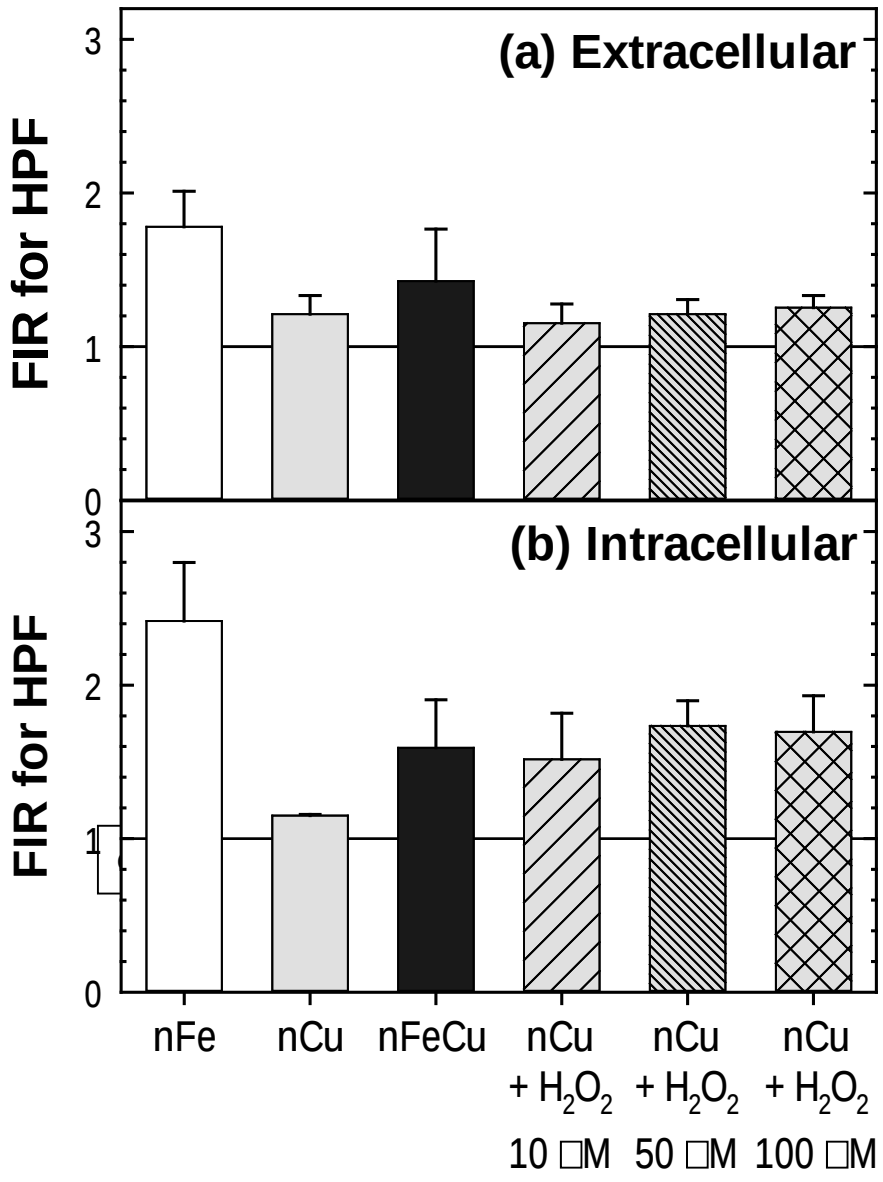

Figure 5.6 (a) Extracellular and (b) intracellular oxidant generation by the zero-valent nanomaterials. ([nFe] = [nCu] = [nFeCu] = 0.05 g/L; [H_2O_2] = 10, 50, 100 μM; $pH_{f, avg.}$ = 6.3; Reaction time = 30 min).

The inactivation of *E. coli* and MS2 coliphage was examined with the same condition of the ROS generation experiment (Figure 5.7). The addition of H_2O_2 to nCu system greatly enhanced the

MS2 inactivation, whereas inhibited *E. coli* inactivation. Increased concentration of H_2O_2 enhanced the inactivation rate of MS2 coliphage by approximately 10-fold, compared to the nCu condition, exceeding the inactivation rate of nFeCu.

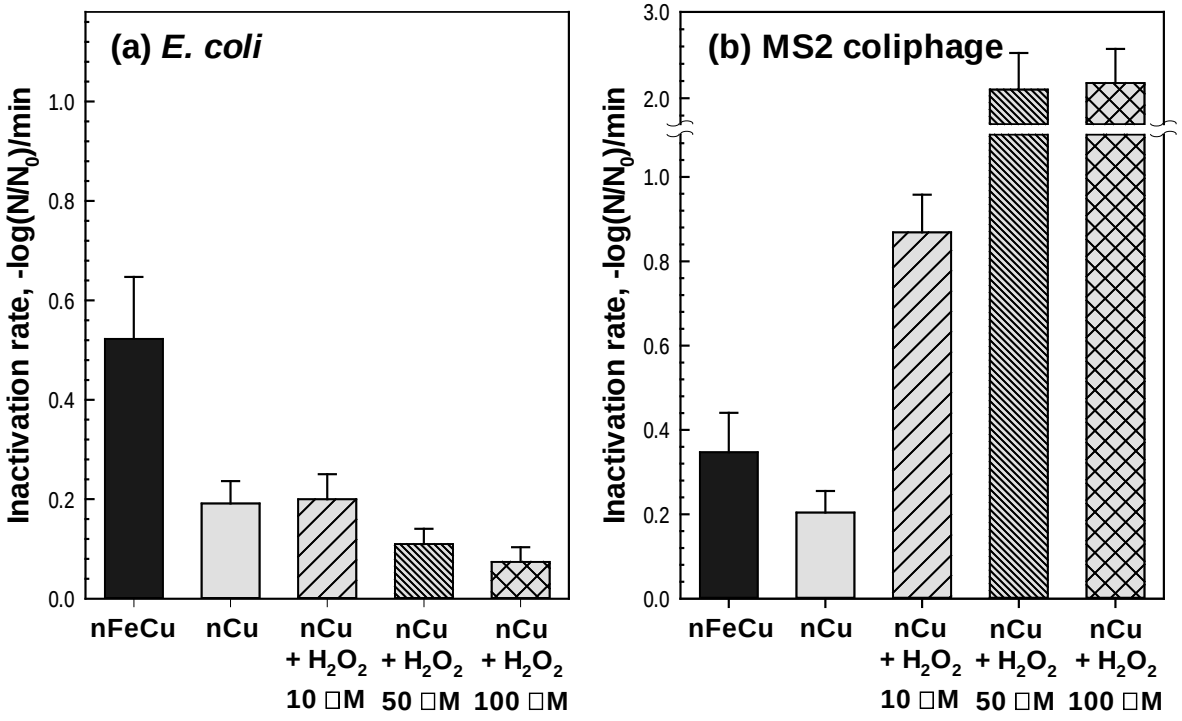

Figure 5.7 Inactivation rate of (a) *E. coli* and (b) MS2 coliphage by the zero-valent nanomaterials with different concentration of H_2O_2. ([nFe] = [nCu] = [nFeCu] = 0.05 g/L; $[H_2O_2]$ = 10, 50, 100 μM; $pH_{f, avg.}$ = 6.3; Reaction time = 30 min).

5.1.5. Measurement of cell viability: Live/Dead cell assay

To understand the relationships between the membrane-damaged cells and inactivation efficiency, *E. coli* cells were stained by the *Bac*Light Live/Dead bacterial viability kit. After inactivation of *E. coli* by NPs, the stained cells were observed by microscope and counted from microscopy images (Figure 5.8) then the ratios of live cells and the inactivation efficiency were determined (Figure 5.9). Microscope images shows that *Bac*Light Live/Dead-stained *E. coli* that were treated by NPs in Figure 4.8a, bimetallic NPs, and nFeCu showed the more membrane-damaged cells.

The decrease of live cell ratio as a function of time showed similar trends with the inactivation efficiency of *E. coli* (Figure 5.3a), in order of nFe, nCu, and nFeCu (Figure 5.8b).

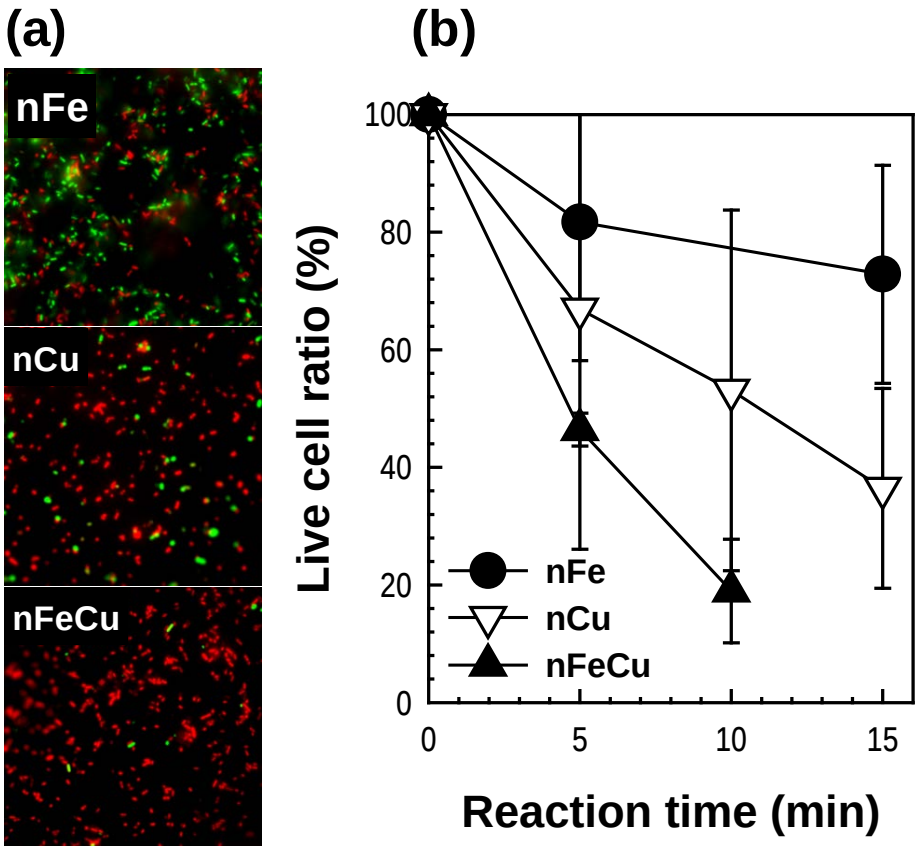

Figure 5.8 Live/Dead *Bac*Light assay: (a) Microscopic images after treatment by the zero-valent nanomaterials, and (b) live cell ratio as a function of time. ([nFe] = [nCu] = [nFeCu] = 0.05 g/L; $pH_{f, avg.}$ = 6.3; Reaction time for microscopic images = 10 min).

The logarithm terms of live-stained cells and that of inactivation efficiency were compared as a function of time (Figure 5.9). A ratio over 1 indicates that the cell membrane is damaged but culturable, while a ratio lower than 1 indicates that the culturable cells are more damaged. As shown in Figure 5.3 and 5.8, nFe damages the cell membrane but cannot damage the culturability of *E. coli*.

However, the NPs with copper-containing materials, nCu and nFeCu, cause cell disruption and induce damage to cell culturablility.

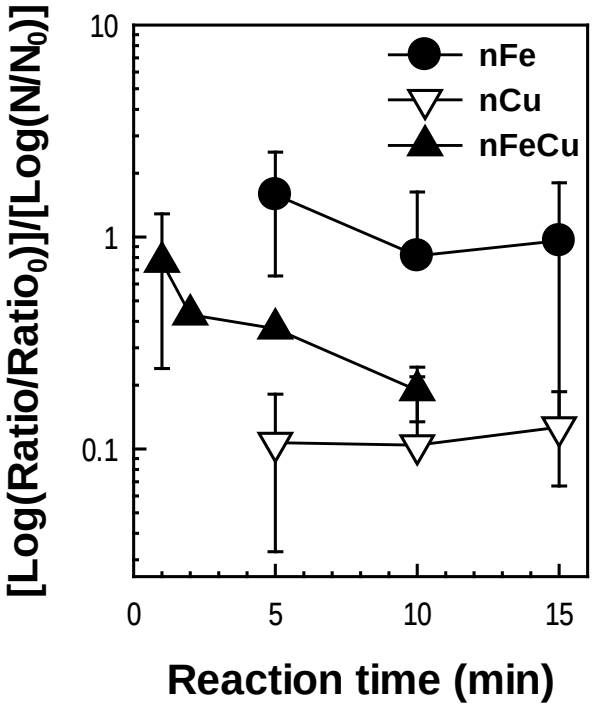

Figure 5.9 Comparison of live cell ratio to the inactivation efficiency of the zero-valent nanomaterials. ([nFe] = [nCu] = [nFeCu] = 0.05 g/L; $pH_{f, avg.}$ = 6.3).

5.1.6. Measurement of damage on virus: Antigenicity and oxidized protein

The reduction of antigenicity and the amount of oxidized proteins of MS2 coliphage inactivated by NPs was determined (Figure 5.10). The changes of antigenicity observed by the absorbance of ELISA kit decreased as a function of time after treatment with various NPs (Figure 5.10a). Unlike the results of inactivation efficiency (Figure 5.4a), the antigenicity of NPs was reduced by 20 to 60% in the order of nFeCu, nFe and nCu after 30 min treatment. nCu was the least effective for the reduction of antigenicity, where the inactivation efficiency was higher than nFe. The antigenicity was not totally reduced by the NPs, the absorbance decreased exponentially with 10-fold serial dilution of MS2 coliphage from 10^8 to 10^3 PFU/mL (5log), and the absorbance by ELISA

analysis was almost not detected with 3log decrease of MS2 coliphage concentration (Figure 5.11). For the reduction of antigenicity, nFe is more effective and the addition of copper somewhat enhanced the efficiency of NPs.

The amount of oxidized proteins of MS2 coliphage was measured by protein carbonyls, which are the common biomarker of protein oxidation (Figure 5.10b) (Dean et al., 1997, Grune et al., 2001). The structure of MS2 coliphage is mainly composed of outer coat protein and the encapsulated RNA (Fiers et al., 1976). The amount of oxidized proteins showed similar trends to the results of the antigenicity experiment (nFeCu > nFe > nCu). The results suggest the greatest loss of antigenicity by protein oxidation. The Fe-based composites (nFeCu and nFe) degrade more effectively, and there are somewhat synergistic effects of copper. Because the RNA is also the protein, PCR experiments were conducted to observe the amount of RNA damage. However, the PCR results showed no inactivation of RNA with Cu-based nanoparticles (nCu and nFeCu) where only nFe showed the degradation of RNA (< 1log, data not shown).

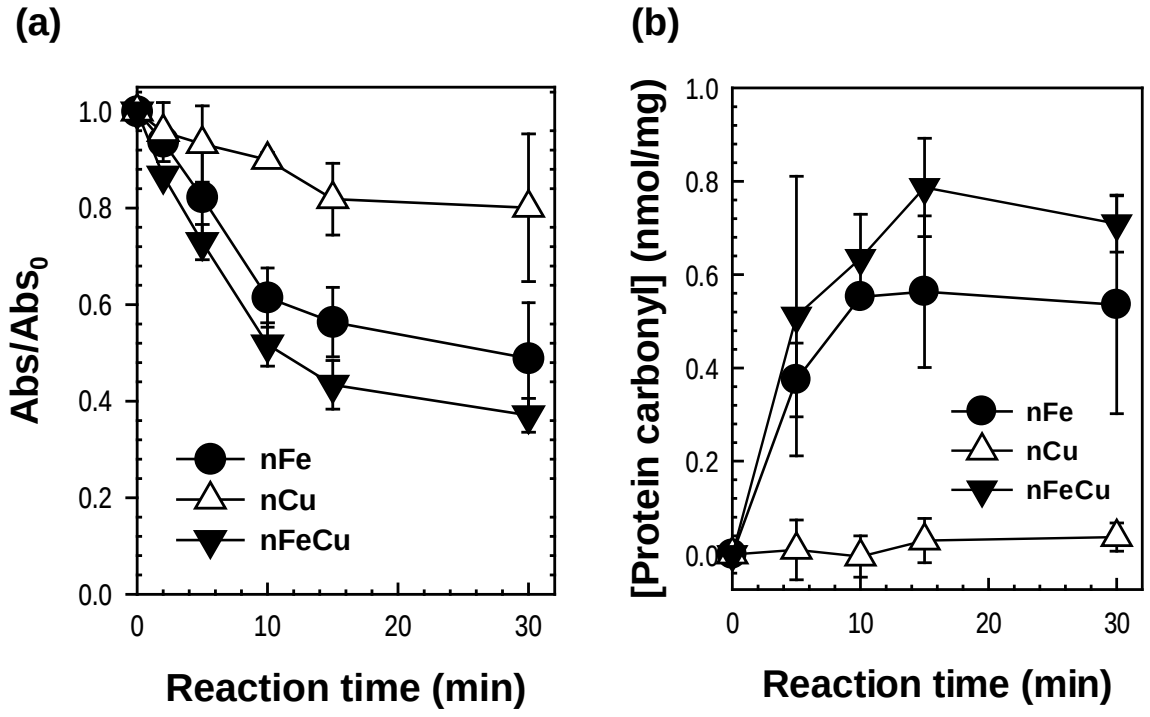

Figure 5.10 (a) Degradation of antigenicity (measured by ELISA) and (b) the amount of oxidized proteins (measured by protein carbonyls) of MS2 coliphage by the zero-valent nanomaterials. ([nFe] = [nCu] = [nFeCu] = 0.05 g/L; $pH_{f, avg.}$ = 6.3).

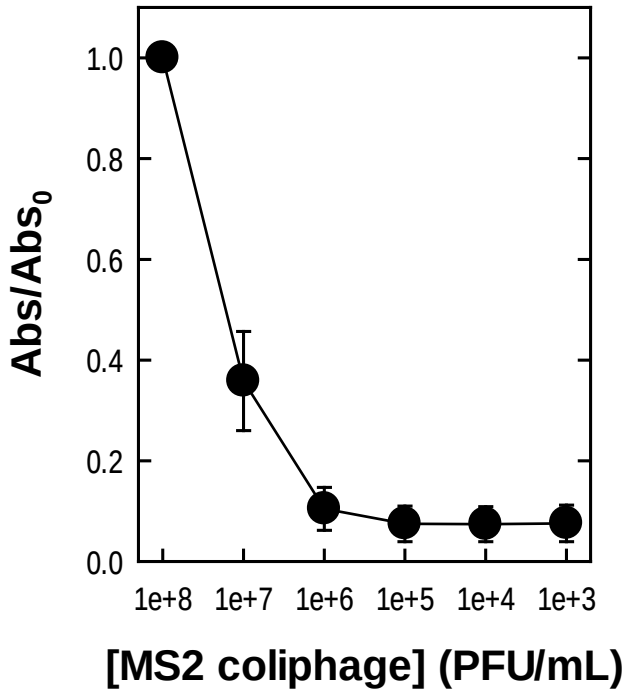

Figure 5.11 Absorbance changes with serial dilution of MS2 coliphage by ELISA analysis

5.2. Discussion

5.2.1. Enhanced biocidal effect of nFeCu

nFeCu showed about 4.5-log inactivation of *E. coli* and MS2 coliphage in 10 min under aerobic condition (Figure 5.3a and 5.4a).Strong bactericidal effect of nFeCu was found under anoxic condition (Figure 5.3b) whereas the virucidal effect of nFeCu under anoxic condition was reduced (Figure 5.4b). This finding indicates that the inactivation mechanism of *E. coli* is different from that of MS2 coliphage. First, in the presence of oxygen, nFe reacts with oxygen to produce Fe(II) and H_2O_2 through a two-electron transfer (Reaction 1). The produced H_2O_2 reacts with copper surface, and leads to the copper-catalyzed Fenton-like reaction with surface-bound Cu(II) producing Cu(I)

(Reaction 2). Previous studies suggested that Cu(I) that is generated by reduction reaction in intracellular cell components is more cytotoxic (Park et al., 2012, Volentini et al., 2011).

$$Fe^0 + O_2 + 2H^+ \rightarrow Fe^{2+} + H_2O_2 \quad (1)$$

$$Cu(II) + H_2O_2 \rightarrow Cu(I) + O_2^{\bullet-} + 2H^+ \quad (2)$$

Second, once the Fenton reaction occurs, nFe and dissolved Fe(II) in bulk and H_2O_2 react and produce $^{\bullet}OH$ or ferryl ion (Fe(IV)) (Reaction 3, 4) (Keenan and Sedlak, 2008, Lee et al., 2008a).

$$Fe^0 + H_2O_2 \rightarrow Fe^{2+} + 2OH^- \quad (3)$$

$$Fe^{2+} + H_2O_2 \rightarrow Fe^{3+} + {}^{\bullet}OH + OH^- \quad \text{or} \quad Fe(IV) + H_2O \quad (4)$$

The addition of copper to the nFe system (the nFeCu system), the production of reactive oxidants varied to another reactive oxidants, Cu(III) (Reaction 5-7) that is capable of causing the oxidative damage to microorganisms (Johnson et al., 1988, Nieto-Juarez et al., 2010).

$$Cu(I) + O_2 \rightarrow Cu(II) + O_2^{\bullet-} \quad (5)$$

$$Cu(I) + O_2^{\bullet-} + 2H^+ \rightarrow Cu(II) + H_2O_2 \quad (6)$$

$$Cu(I) + H_2O_2 \rightarrow Cu(II) + {}^{\bullet}OH + OH^- \quad \text{or} \quad Cu(III) + 2OH^- \quad (7)$$

Previous researchers have demonstrated that reactive oxidants produced from the Fenton or Fenton-like system (i.e., $^{\bullet}OH$, Fe(IV), or Cu(III)) in neutral pH showed biocidal effects (Kim et al., 2015, Nguyen et al., 2013, Kim et al., 2010b, Kim et al., 2011).

5.2.2. Inactivation of *E. coli*

The bactericidal action of the nFeCu system is mainly achieved by Cu(I), which has cytotoxicity to *E. coli*. The enhanced inactivation efficiency of nFeCu was observed under both oxic and anoxic conditions, compared to nFe or nCu (Figure 5.3). Under anoxic condition, nFe and nFeCu show great enhancement of the inactivation of *E. coli*, the color in the reactor changing from blackish to yellow, as Fe(III) was produced under oxic condition. These results are consistent with the previous observation (Lee et al., 2008b), the oxidation of nFe inhibited biocidal activity. The greater content ratio of iron to copper in nFeCu, Fe(II) also induced intracellular oxidative stress by producing

reactive oxidant species from reaction with intracellular O_2 or H_2O_2. Moreover, anoxic condition prevented the oxidation of Cu(I) by oxygen (Reaction 5), showing that the nFeCu system can achieve the relatively higher inactivation of *E. coli*.

The inactivation rate of the nFeCu shows that there is not significantscavenging by MeOH that is applied as reactive oxidants scavenger, while the copper-chelating scavengers, DMP and EDTA, eliminate the biocidal activity (Figure 5.5a). NPs naturally release iron or copper ion or form surface-bounded ions. For this reason, the nCu can inactivate *E. coli* under the anoxic condition by the redox cycling reaction between Cu(I) and Cu(II) (Santo et al., 2008). The scavenging effects of copper-chelating reagents were significant under the anoxic condition (data not shown) that refer to the Cu(I) being the main bactericide. However, the nCu/H_2O_2 system had no enhancement of inactivation efficacy on *E. coli* even with the increase of H_2O_2 addition (Figure 5.7), even though the system can produce reactive oxidants such as $^{\bullet}$OH or Cu(III) by the copper-catalyzed Fenton-like system (Reaction 7).

In the previous study, Cu(I) does not significantly disrupt the integrity of cell membranes (Kim et al., 2015). The enhanced inactivation of *E. coli* by nFeCu is not derived from damaging of the cell membrane that was indicated from the Bac*Light* Live/Dead assay. Even though the live cell ratio degradation by the NPs showed similar trend to the inactivation efficiency (Figure 5.8b), the calculated ratio from the live cell ratio versus the inactivation efficiency indicates that the induced damage by copper-include NPs relates more to cytoplasmic damage. It was reported that the aggregation of nFeCu was accumulated in the periplasm, and caused significant ruptures at various sites in the membrane (Kim et al., 2014).

5.2.3. Inactivation of MS2 coliphage

In contrast with the *E. coli* inactivation, reactive oxidants (i.e. Cu(III), $^{\bullet}$OH or Fe(IV)) appear to play important roles in the MS2 coliphage inactivation. Under the anoxic condition, the inactivation was notably decreased, compared to the oxic condition (Figure 5.4).

Radical scavenger, MeOH partially scavenged the inactivation efficiency of nFeCu, where DMP did not show significant scavenging effect compared to MeOH. DMP is known as a Cu(I)-chelating reagent, while the effective reactive oxidant species for inactivation of MS2 coliphage is iron-induced reactive oxidants ($^{\bullet}$OH or Fe(IV)). Possible interactions between Fe(II) (or nZVI) and the amino acids in the protein capsid of MS2 coliphage may also enhance the selectivity of Fe(IV)

toward MS2 coliphage. In particular, the addition of H_2O_2 to nCu somewhat increases the generated fluorescence intensity at cell-free condition (Figure 5.6a) and the inactivation efficiency of MS2 coliphage was dramatically enhanced (Figure 5.7b). This implies that MS2 coliphage is sensitive to the oxidative damage induced by reactive oxidants.

However, the reduction of antigenicity of MS2 coliphage by the NPs showed different trends (Figure 5.10a). ELISA analysis has been used to examine the disinfection mechanism of viruses, since the reactivity of antibodies with virus is likely to depend upon how an intact protein capsid is altered by disinfectants. The integrity of MS2 coliphage was reduced by nFe causing more damage to the external capsid (Kim et al., 2011). This study, it is clarified that damage of capsid occurred by the NPs, but it is hard to define which reactive oxidant (Fe- or Cu-induced reactive oxidants) is more effective for antigenicity degradation. As mentioned above, MS2 coliphage consists with the outer coat protein, and encapsulated RNA. Therefore, the results of oxidized protein (Figure 5.10b) and PCR (data not shown) were expected. Further studies are required to determine the difference of MS2 coliphage inactivation mechanisms between the Fe- and Cu-originated reactive oxidants.

CHAPTER 6.

Conclusions

Copper is essentially required for living species, but has also in many respects exhibited antimicrobial efficacy. In this study, the antimicrobial effects of the copper-based disinfection systems were investigated in neutral pH and natural waters and the inactivation mechanism was elucidated. The copper-based disinfection systems suggested in this work would be promising systems that are effective for bacteria and viruses without producing disinfectant by-products (DBPs).

The Cu(II)/HA system has potential applications as a disinfection technology for many water uses such as wastewater, reused water, industrial and agricultural water, and possibly drinking water; note that significant inactivation of bacteria and viruses was achieved by relatively low concentrations of reagents (usually micromolar levels of Cu(II), HA, and H_2O_2). The concentration of Cu(II) used in this study (5 μM) is even lower than the WHO drinking water guideline value (2 mg/L = 31.4 μM (WHO)) and the drinking water standards in the United States (1.3 mg/L = 20.5 μM (USEPA, 2007)) and in Korea (1 mg/L = 15.7 μM (Ministry of Environment, Republic of Korea)). The Cu(II)/HA system exhibited substantial activity in natural water even if the disinfection efficacy was somewhat decreased by manifold factors (e.g., copper-chelation, oxidant scavenging, and undesired consumption of HA by natural organic and inorganic substances). In particular, the employment of H_2O_2 in the Cu(II)/HA system (i.e., the Cu(II)/HA/H_2O_2 system) showed excellent virucidal activity (> 4log inactivation of MS2 coliphage in 1 min), implying that the Cu(II)/HA/H_2O_2 system can be successfully applied for special purposes needing the control of viral strains. A concern regarding the potential toxicity of HA may be raised. However, HA was completely decomposed within minutes, and no residual HA was detected after the reaction (data not shown). For better application of the Cu(II)/HA system, impacts of various substances from different water matrices need to be studied further. The development of heterogeneous systems utilizing immobilized copper compounds will also be beneficial.

The copper-catalyzed PMS clearly shows the inactivation efficiency on *E. coli* and MS2 coliphage in natural water and has potential applications as a disinfection technology. However, further studies are needed to understand the inactivation mechanisms of virus by the Cu(II)/PMS system, and to optimize the concentration and injection of additives. In addition, the water quality can

also be an important factor; that pH, alkalinity, and natural organic matters (NOMs) can inhibit the production of reactive oxidant species. In particular, the effect of Suwannee river humic acid, a common alternate of NOM, was tested in pH-controlled deionized water (data not shown); the efficacy of the Cu(II)/PMS system decreased with elevated concentration of humic acid.

The utilization of copper to catalyze PMS was studied in different types of species, ion (Fernandez et al., 2004, Kumar et al., 2012) and heterogeneous catalysts (Ding et al., 2013, Feng et al., 2016, Lei et al., 2015) for degradation of organic compounds. All this, as well as disinfection can be of general application, expanding the application spectrum, and immobilized heterogeneous catalysts can be alternative suppliers of copper releasing source.

nFeCu is a promising antimicrobial material that exhibits stronger bactericidal and virucidal properties than nFe or nCu. nFeCu is more applicable to bacteria inactivation than to virus inactivation in both aerobic and anaerobic condition, whereas the anaerobic condition enhanced the bactericidal activity. It is easy to synthesize, adding $CuSO_4$ solution as required after preparation of nZVI suspension. Compared to the bare nZVI, the addition of only a small amount of copper (< 10%) provides great enhancement in biocidal activity, and comparatively, it is less oxidized than nZVI. The material was possible to keep in the ambient condition, and the biocidal effect would last for at least 6 months. Another advantage of the nFeCu is that it can be possible to immobilize onto various support materials, rather than adding as ions.

REFERENCES

ANDERSON, J. H. 1964. The copper-catalysed oxidation of hydroxylamine. *Analyst,* 89**,** 357-362.

ANIPSITAKIS, G. P. & DIONYSIOU, D. D. 2003. Degradation of Organic Contaminants in Water with Sulfate Radicals Generated by the Conjunction of Peroxymonosulfate with Cobalt. *Environmental Science & Technology,* 37**,** 4790-4797.

ANIPSITAKIS, G. P. & DIONYSIOU, D. D. 2004. Radical Generation by the Interaction of Transition Metals with Common Oxidants. *Environmental Science & Technology,* 38**,** 3705-3712.

ANIPSITAKIS, G. P., TUFANO, T. P. & DIONYSIOU, D. D. 2008. Chemical and microbial decontamination of pool water using activated potassium peroxymonosulfate. *Water Research,* 42**,** 2899-2910.

AUFFAN, M., ACHOUAK, W., ROSE, J., RONCATO, M.-A., CHAN AC, C., WAITE, D. T., MASION, A., WOICIK, J. C., WIESNER, M. R. & BOTTERO, J.-Y. 2008. Relation between the Redox State of Iron-Based Nanoparticles and Their Cytotoxicity toward Escherichia coli. *Environmental Science & Technology,* 42**,** 6730-6735.

AZAM, A., AHMED, A. S., OVES, M., KHAN, M. S., HABIB, S. S. & MEMIC, A. 2012. Antimicrobial activity of metal oxide nanoparticles against Gram-positive and Gram-negative bacteria: a comparative study. *International Journal of Nanomedicine,* 7**,** 6003-6009.

BATAINEH, H., PESTOVSKY, O. & BAKAC, A. 2012. pH-induced mechanistic changeover from hydroxyl radicals to iron(iv) in the Fenton reaction. *Chemical Science,* 3**,** 1594-1599.

BERNASCONI, L. & BAERENDS, E. J. 2009. Generation of Ferryl Species through Dioxygen Activation in Iron/EDTA Systems: A Computational Study. *Inorganic Chemistry,* 48**,** 527-540.

BESWICK, P. H., HALL, G. H., HOOK, A. J., LITTLE, K., MCBRIEN, D. C. H. & LOTT, K. A. K. 1976. Copper toxicity: Evidence for the conversion of cupric to cuprous copper in vivo under anaerobic conditions. *Chemico-Biological Interactions,* 14**,** 347-356.

BONDARENKO, O., JUGANSON, K., IVASK, A., KASEMETS, K., MORTIMER, M. & KAHRU, A. 2013. Toxicity of Ag, CuO and ZnO nanoparticles to selected environmentally relevant test organisms and mammalian cells in vitro: a critical review. *Archives of Toxicology,* 87**,** 1181-1200.

BORKOW, G., SIDWELL, R. W., SMEE, D. F., BARNARD, D. L., MORREY, J. D., LARA-VILLEGAS, H. H., SHEMER-AVNI, Y. & GABBAY, J. 2007. Neutralizing Viruses in Suspensions by Copper Oxide-Based Filters. *Antimicrobial Agents and Chemotherapy,* 51**,** 2605-2607.

BUXTON, G. V., GREENSTOCK, C. L., HELMAN, W. P. & ROSS, A. B. 1988. Critical Review of rate constants for reactions of hydrated electrons, hydrogen atoms and hydroxyl radicals (·OH/·O− in Aqueous Solution. *Journal of Physical and Chemical Reference Data,* 17**,** 513-886.

CHO, M., LEE, J., MACKEYEV, Y., WILSON, L. J., ALVAREZ, P. J. J., HUGHES, J. B. & KIM, J.-H. 2010. Visible Light Sensitized Inactivation of MS-2 Bacteriophage by a Cationic Amine-Functionalized C60 Derivative. *Environmental Science & Technology,* 44**,** 6685-6691.

CIOFFI, N., TORSI, L., DITARANTO, N., TANTILLO, G., GHIBELLI, L., SABBATINI, L., BLEVE-ZACHEO, T., D'ALESSIO, M., ZAMBONIN, P. G. & TRAVERSA, E. 2005. Copper Nanoparticle/Polymer Composites with Antifungal and Bacteriostatic Properties. *Chemistry of Materials,* 17**,** 5255-5262.

CRIST, R. H., OBERHOLSER, K., SCHWARTZ, D., MARZOFF, J., RYDER, D. & CRIST, D. R. 1988. Interactions of metals and protons with algae. *Environmental Science & Technology,* 22**,** 755-760.

DANKOVICH, T. A. & SMITH, J. A. 2014. Incorporation of copper nanoparticles into paper for point-of-use water purification. *Water Research,* 63**,** 245-251.

DE LAAT, J. & GALLARD, H. 1999. Catalytic Decomposition of Hydrogen Peroxide by Fe(III) in Homogeneous Aqueous Solution: Mechanism and Kinetic Modeling. *Environmental Science & Technology,* 33**,** 2726-2732.

DE SCHAMPHELAERE, K. A. C. & JANSSEN, C. R. 2002. A Biotic Ligand Model Predicting Acute Copper Toxicity for Daphnia magna: The Effects of Calcium, Magnesium, Sodium, Potassium, and pH. *Environmental Science & Technology,* 36**,** 48-54.

DEAN, R. T., FU, S., STOCKER, R. & DAVIES, M. J. 1997. Biochemistry and pathology of radical-mediated protein oxidation. *Biochemical Journal,* 324**,** 1-18.

DING, Y., ZHU, L., WANG, N. & TANG, H. 2013. Sulfate radicals induced degradation of tetrabromobisphenol A with nanoscaled magnetic CuFe2O4 as a heterogeneous catalyst of peroxymonosulfate. *Applied Catalysis B: Environmental,* 129**,** 153-162.

DIZAJ, S. M., LOTFIPOUR, F., BARZEGAR-JALALI, M., ZARRINTAN, M. H. & ADIBKIA, K. 2014. Antimicrobial activity of the metals and metal oxide nanoparticles. *Materials Science and Engineering: C,* 44**,** 278-284.

EATON, A. D., FRANSON, M. A. H., ASSOCIATION, A. P. H., ASSOCIATION, A. W. W. & FEDERATION, W. E. 2005. *Standard Methods for the Examination of Water & Wastewater*, American Public Health Association.

FENG, Q., WU, J., CHEN, G., CUI, F., KIM, T. & KIM, J. 2000. A mechanistic study of the antibacterial effect of silver ions on Escherichia coli and Staphylococcus aureus. *Journal of biomedical materials research,* 52**,** 662-668.

FENG, Y., WU, D., DENG, Y., ZHANG, T. & SHIH, K. 2016. Sulfate Radical-Mediated Degradation of Sulfadiazine by CuFeO2 Rhombohedral Crystal-Catalyzed Peroxymonosulfate: Synergistic Effects and Mechanisms. *Environmental Science & Technology,* 50**,** 3119-3127.

FERNANDEZ, J., MARUTHAMUTHU, P. & KIWI, J. 2004. Photobleaching and mineralization of Orange II by oxone and metal-ions involving Fenton-like chemistry under visible light. *Journal of Photochemistry and Photobiology A: Chemistry,* 161**,** 185-192.

FIERS, W., CONTRERAS, R., DUERINCK, F., HAEGEMAN, G., ISERENTANT, D., MERREGAERT, J., MIN JOU, W., MOLEMANS, F., RAEYMAEKERS, A., VAN DEN

BERGHE, A., VOLCKAERT, G. & YSEBAERT, M. 1976. Complete nucleotide sequence of bacteriophage MS2 RNA: primary and secondary structure of the replicase gene. *Nature,* 260**,** 500-507.

GILBERT, B. C. & STELL, J. K. 1990. Mechanisms of peroxide decomposition. An ESR study of the reactions of the peroxomonosulphate anion (HOOSO3-) with Ti, Fe, and [small alpha]-oxygen-substituted radicals. *Journal of the Chemical Society, Perkin Transactions 2***,** 1281-1288.

GOMES, A., FERNANDES, E. & LIMA, J. L. F. C. 2005. Fluorescence probes used for detection of reactive oxygen species. *Journal of Biochemical and Biophysical Methods,* 65**,** 45-80.

GRUNE, T., KLOTZ, L.-O., GIECHE, J., RUDECK, M. & SIES, H. 2001. Protein oxidation and proteolysis by the nonradical oxidants singlet oxygen or peroxynitrite. *Free Radical Biology and Medicine,* 30**,** 1243-1253.

HOSSAIN, F., PERALES-PEREZ, O. J., HWANG, S. & ROM N, F. 2014. Antimicrobial nanomaterials as water disinfectant: Applications, limitations and future perspectives. *Science of The Total Environment,* 466–467**,** 1047-1059.

HUANG, L., LI, D.-Q., LIN, Y.-J., WEI, M., EVANS, D. G. & DUAN, X. 2005. Controllable preparation of Nano-MgO and investigation of its bactericidal properties. *Journal of Inorganic Biochemistry,* 99**,** 986-993.

HUIE, R. E., CLIFTON, C. L. & NETA, P. 1991. Electron transfer reaction rates and equilibria of the carbonate and sulfate radical anions. *International Journal of Radiation Applications and Instrumentation. Part C. Radiation Physics and Chemistry,* 38**,** 477-481.

ITO, K. & KAWANISHI, S. 1991. Site-specific fragmentation and modification of albumin by sulfite in the presence of metal ions or peroxidase/H2O2: Role of sulfate radical. *Biochemical and Biophysical Research Communications,* 176**,** 1306-1312.

JOHNSON, G. R. A., NAZHAT, N. B. & SAADALLA-NAZHAT, R. A. 1988. Reaction of the aquacopper(I) ion with hydrogen peroxide. Evidence for a Cu^{III}(cupryl) intermediate. *Journal of the Chemical Society, Faraday Transactions 1: Physical Chemistry in Condensed Phases,* 84**,** 501-510.

JONES, N., RAY, B., RANJIT, K. T. & MANNA, A. C. 2008. Antibacterial activity of ZnO nanoparticle suspensions on a broad spectrum of microorganisms. *FEMS Microbiology Letters,* 279**,** 71.

JOO, S. H., FEITZ, A. J., SEDLAK, D. L. & WAITE, T. D. 2005. Quantification of the Oxidizing Capacity of Nanoparticulate Zero-Valent Iron. *Environmental Science & Technology,* 39**,** 1263-1268.

JOO, S. H., FEITZ, A. J. & WAITE, T. D. 2004. Oxidative Degradation of the Carbothioate Herbicide, Molinate, Using Nanoscale Zero-Valent Iron. *Environmental Science & Technology,* 38**,** 2242-2247.

JOSE RUBEN, M., JOSE LUIS, E., ALEJANDRA, C., KATHERINE, H., JUAN, B. K., JOSE TAPIA, R. & MIGUEL JOSE, Y. 2005. The bactericidal effect of silver nanoparticles. *Nanotechnology,* 16**,** 2346.

KEENAN, C. R. & SEDLAK, D. L. 2008. Factors Affecting the Yield of Oxidants from the Reaction of Nanoparticulate Zero-Valent Iron and Oxygen. *Environmental Science & Technology,* 42**,** 1262-1267.

KIM, E.-J., LE THANH, T. & CHANG, Y.-S. 2014. Comparative toxicity of bimetallic Fe nanoparticles toward Escherichia coli: mechanism and environmental implications. *Environmental Science: Nano,* 1**,** 233-237.

KIM, H.-E., NGUYEN, T. T. M., LEE, H. & LEE, C. 2015. Enhanced Inactivation of Escherichia coli and MS2 Coliphage by Cupric Ion in the Presence of Hydroxylamine: Dual Microbicidal Effects. *Environmental Science & Technology,* 49**,** 14416-14423.

KIM, J. Y., LEE, C., LOVE, D. C., SEDLAK, D. L., YOON, J. & NELSON, K. L. 2011. Inactivation of MS2 Coliphage by Ferrous Ion and Zero-Valent Iron Nanoparticles. *Environmental Science & Technology,* 45**,** 6978-6984.

KIM, J. Y., LEE, C., SEDLAK, D. L., YOON, J. & NELSON, K. L. 2010a. Inactivation of MS2 coliphage by Fenton's reagent. *Water Research,* 44**,** 2647-2653.

KIM, J. Y., PARK, H.-J., LEE, C., NELSON, K. L., SEDLAK, D. L. & YOON, J. 2010b. Inactivation of Escherichia coli by Nanoparticulate Zerovalent Iron and Ferrous Ion. *Applied and Environmental Microbiology,* 76**,** 7668-7670.

KIMURA, T. & NISHIOKA, H. 1997. Intracellular generation of superoxide by copper sulphate in *Escherichia coli*. *Mutation Research/Genetic Toxicology and Environmental Mutagenesis,* 389**,** 237-242.

KIRAKOSYAN, G., TRCHOUNIAN, K., VARDANYAN, Z. & TRCHOUNIAN, A. 2008. mCopper (II) Ions Affect *Escherichia coli* Membrane Vesicles' SH-Groups and a Disulfide-Dithiol Interchange Between Membrane Proteins. *Cell Biochemistry and Biophysics,* 51**,** 45-50.

Ministry of Environment, Republic of KOREA, 2014. Available: www.me.go.kr [Accessed].

KUMAR, P. S., RAJ, R. M., RANI, S. K. & EASWARAMOORTHY, D. 2012. Reaction Kinetics and Mechanism of Copper(II) Catalyzed Oxidative Deamination and Decarboxylation of Ornithine by Peroxomonosulfate. *Industrial & Engineering Chemistry Research,* 51**,** 6310-6319.

LEE, C., KEENAN, C. R. & SEDLAK, D. L. 2008a. Polyoxometalate-Enhanced Oxidation of Organic Compounds by Nanoparticulate Zero-Valent Iron and Ferrous Ion in the Presence of Oxygen. *Environmental Science & Technology,* 42**,** 4921-4926.

LEE, C., KIM, J. Y., LEE, W. I., NELSON, K. L., YOON, J. & SEDLAK, D. L. 2008b. Bactericidal Effect of Zero-Valent Iron Nanoparticles on Escherichia coli. *Environmental Science & Technology,* 42**,** 4927-4933.

LEE, H.-J., LEE, H. & LEE, C. 2014. Degradation of diclofenac and carbamazepine by the copper(II)-catalyzed dark and photo-assisted Fenton-like systems. *Chemical Engineering Journal,* 245**,** 258-264.

LEE, H., LEE, H.-J., SEDLAK, D. L. & LEE, C. 2013. pH-Dependent reactivity of oxidants formed by iron and copper-catalyzed decomposition of hydrogen peroxide. *Chemosphere,* 92**,** 652-658.

LEI, Y., CHEN, C.-S., TU, Y.-J., HUANG, Y.-H. & ZHANG, H. 2015. Heterogeneous Degradation of Organic Pollutants by Persulfate Activated by CuO-Fe3O4: Mechanism, Stability, and Effects of pH and Bicarbonate Ions. *Environmental Science & Technology,* 49**,** 6838-6845.

LEMIRE, J. A., HARRISON, J. J. & TURNER, R. J. 2013. Antimicrobial activity of metals: mechanisms, molecular targets and applications. *Nat Rev Micro,* 11**,** 371-384.

LENTE, G., KALM R, J., BARANYAI, Z., KUN, A., K K, I., BAJUSZ, D., TAK CS, M., VERES, L. & F BI N, I. 2009. One- Versus Two-Electron Oxidation with Peroxomonosulfate Ion: Reactions with Iron(II), Vanadium(IV), Halide Ions, and Photoreaction with Cerium(III). *Inorganic Chemistry,* 48**,** 1763-1773.

LI, L., FAN, M., BROWN, R. C., VAN LEEUWEN, J., WANG, J., WANG, W., SONG, Y. & ZHANG, P. 2006. Synthesis, Properties, and Environmental Applications of Nanoscale Iron-Based Materials: A Review. *Critical Reviews in Environmental Science and Technology,* 36**,** 405-431.

LI, Q., MAHENDRA, S., LYON, D. Y., BRUNET, L., LIGA, M. V., LI, D. & ALVAREZ, P. J. J. 2008. Antimicrobial nanomaterials for water disinfection and microbial control: Potential applications and implications. *Water Research,* 42**,** 4591-4602.

MAHAPATRA, O., BHAGAT, M., GOPALAKRISHNAN, C. & ARUNACHALAM, K. D. 2008. Ultrafine dispersed CuO nanoparticles and their antibacterial activity. *Journal of Experimental Nanoscience,* 3**,** 185-193.

MARKOV , Z., ŠIŠKOV , K. N. M., FILIP, J., ČUDA, J., KOL Ř, M., ŠAF ŘOV , K., MEDŘ K, I. & ZBOŘIL, R. 2013. Air Stable Magnetic Bimetallic Fe–Ag Nanoparticles for Advanced Antimicrobial Treatment and Phosphorus Removal. *Environmental Science & Technology,* 47**,** 5285-5293.

MCCARTHY, T. J., ZEELIE, J. J. & KRAUSE, D. J. 1992. The antimicrobial action of zinc ion/antioxidant combinations. *Journal of Clinical Pharmacy and Therapeutics,* 17**,** 51-54.

MIDANDER, K., CRONHOLM, P., KARLSSON, H. L., ELIHN, K., M LLER, L., LEYGRAF, C. & WALLINDER, I. O. 2009. Surface Characteristics, Copper Release, and Toxicity of Nano- and Micrometer-Sized Copper and Copper(II) Oxide Particles: A Cross-Disciplinary Study. *Small,* 5**,** 389-399.

NAGARAJAN, P. & RAJAGOPALAN, V. 2008. Enhanced bioactivity of ZnO nanoparticles—an antimicrobial study. *Science and Technology of Advanced Materials,* 9**,** 035004.

NAIR, S., SASIDHARAN, A., DIVYA RANI, V. V., MENON, D., NAIR, S., MANZOOR, K. & RAINA, S. 2008. Role of size scale of ZnO nanoparticles and microparticles on toxicity toward bacteria and osteoblast cancer cells. *Journal of Materials Science: Materials in Medicine,* 20**,** 235.

NETA, P., HUIE, R. E. & ROSS, A. B. 1988. Rate Constants for Reactions of Inorganic Radicals in Aqueous Solution. *Journal of Physical and Chemical Reference Data,* 17**,** 1027-1284.

NGUYEN, T. T. M., PARK, H.-J., KIM, J. Y., KIM, H.-E., LEE, H., YOON, J. & LEE, C. 2013. Microbial Inactivation by Cupric Ion in Combination with H2O2: Role of Reactive Oxidants. *Environmental Science & Technology,* 47**,** 13661-13667.

NIETO-JUAREZ, J. I., PIERZCHŁA, K., SIENKIEWICZ, A. & KOHN, T. 2010. Inactivation of MS2 coliphage in Fenton and Fenton-like systems: role of transition metals, hydrogen peroxide and sunlight. *Environmental Science & Technology,* 44**,** 3351-3356.

OHSUMI, Y., KITAMOTO, K. & ANRAKU, Y. 1988. Changes induced in the permeability barrier of the yeast plasma membrane by cupric ion. *Journal of Bacteriology,* 170**,** 2676-2682.

PARK, H.-J., NGUYEN, T. T. M., YOON, J. & LEE, C. 2012. Role of Reactive Oxygen Species in Escherichia coli Inactivation by Cupric Ion. *Environmental Science & Technology,* 46**,** 11299-11304.

PATIKARNMONTHON, N., NAWAPAN, S., BURANAJITPAKORN, S., CHAROENLAP, N., MONGKOLSUK, S. & VATTANAVIBOON, P. 2010. Copper ions potentiate organic hydroperoxide and hydrogen peroxide toxicity through different mechanisms in Xanthomonas campestris pv. campestris. *FEMS Microbiology Letters,* 313**,** 75-80.

PHAM, A. N., XING, G., MILLER, C. J. & WAITE, T. D. 2013. Fenton-like copper redox chemistry revisited: Hydrogen peroxide and superoxide mediation of copper-catalyzed oxidant production. *Journal of Catalysis,* 301**,** 54-64.

RUPARELIA, J. P., CHATTERJEE, A. K., DUTTAGUPTA, S. P. & MUKHERJI, S. 2008. Strain specificity in antimicrobial activity of silver and copper nanoparticles. *Acta Biomaterialia,* 4**,** 707-716.

SAGRIPANTI, J. L., ROUTSON, L. B. & LYTLE, C. D. 1993. Virus inactivation by copper or iron ions alone and in the presence of peroxide. *Applied and Environmental Microbiology,* 59**,** 4374-4376.

SANTO, C. E., TAUDTE, N., NIES, D. H. & GRASS, G. 2008. Contribution of Copper Ion Resistance to Survival of Escherichia coli on Metallic Copper Surfaces. *Applied and Environmental Microbiology,* 74**,** 977-986.

SEIL, J. T. & WEBSTER, T. J. 2012. Antimicrobial applications of nanotechnology: methods and literature. *International Journal of Nanomedicine,* 7**,** 2767-2781.

SHI, L.-E., XING, L., HOU, B., GE, H., GUO, X. & TANG, Z. 2010. Inorganic nano mental oxides used as anti-microorganism agents for pathogen control. *Current Research, Technology and Education Topics in Applied Microbiology and Microbial***,** 361-368.

SIMON-DECKERS, A., LOO, S., MAYNE-L'HERMITE, M., HERLIN-BOIME, N., MENGUY, N., REYNAUD, C., GOUGET, B. & CARRI RE, M. 2009. Size-, Composition- and Shape-Dependent Toxicological Impact of Metal Oxide Nanoparticles and Carbon Nanotubes toward Bacteria. *Environmental Science & Technology,* 43**,** 8423-8429.

SMITH, R. C. & REED, V. D. 1992. Inhibition by thiols of copper(II)-induced oxidation of oxyhemoglobin. *Chemico-Biological Interactions,* 82**,** 209-217.

SONDI, I. & SALOPEK-SONDI, B. 2004. Silver nanoparticles as antimicrobial agent: a case study on E. coli as a model for Gram-negative bacteria. *Journal of Colloid and Interface Science,* 275**,** 177-182.

STERRITT, R. M. & LESTER, J. N. 1980. Interactions of heavy metals with bacteria. *Science of The Total Environment,* 14**,** 5-17.

STOHS, S. J. & BAGCHI, D. 1995. Oxidative mechanisms in the toxicity of metal ions. *Free Radical Biology and Medicine,* 18**,** 321-336.

SUN, Y.-P., LI, X.-Q., CAO, J., ZHANG, W.-X. & WANG, H. P. 2006. Characterization of zero-valent iron nanoparticles. *Advances in Colloid and Interface Science,* 120**,** 47-56.

TAYLOR, E. N. & WEBSTER, T. J. 2009. The use of superparamagnetic nanoparticles for prosthetic biofilm prevention. *International Journal of Nanomedicine,* 4**,** 145-152.

TOMAT, R., RIGO, A. & SALMASO, R. 1975. Kinetic study on the reaction between O_2 and hydroxylamine. *Journal of Electroanalytical Chemistry and Interfacial Electrochemistry,* 59**,** 255-260.

TRAN, N., MIR, A., MALLIK, D., SINHA, A., NAYAR, S. & WEBSTER, T. J. 2010. Bactericidal effect of iron oxide nanoparticles on Staphylococcus aureus. *International Journal of Nanomedicine,* 5**,** 277-283.

USEPA. 2007. *Drinking water regulations: maximum contaminant level goals and national primary drinking water regulations for lead and copper* [Online]. Available: www.epa.gov [Accessed].

VALODKAR, M., MODI, S., PAL, A. & THAKORE, S. 2011. Synthesis and anti-bacterial activity of Cu, Ag and Cu–Ag alloy nanoparticles: A green approach. *Materials Research Bulletin,* 46**,** 384-389.

VOLENTINI, S. I., FAR AS, R. N., RODR GUEZ-MONTELONGO, L. & RAPISARDA, V. A. 2011. Cu(II)-reduction by Escherichia coli cells is dependent on respiratory chain components. *BioMetals,* 24**,** 827-835.

WALLING, C. & GOOSEN, A. 1973. Mechanism of the ferric ion catalyzed decomposition of hydrogen peroxide. Effect of organic substrates. *Journal of the American Chemical Society,* 95**,** 2987-2991.

WANG, Q., KANEL, S. R., PARK, H., RYU, A. & CHOI, H. 2008. Controllable synthesis, characterization, and magnetic properties of nanoscale zerovalent iron with specific high Brunauer–Emmett–Teller surface area. *Journal of Nanoparticle Research,* 11**,** 749-755.

WOO, H., PARK, J., LEE, S. & LEE, S. 2014. Effects of washing solution and drying condition on reactivity of nano-scale zero valent irons (nZVIs) synthesized by borohydride reduction. *Chemosphere,* 97**,** 146-152.

WORLD HEALTH ORGANIZATION, 2004. *Guidelines for drinking-water quality* [Online]. Geneva: World Health Organization. Available: http://www.myilibrary.com?id=9744 [Accessed].

YAMAMOTO, N., HIATT, C. W. & HALLER, W. 1964. Mechanism of inactivation of bacteriophages by metals. *Biochimica et Biophysica Acta (BBA) - Specialized Section on Nucleic Acids and Related Subjects,* 91**,** 257-261.

YAMAMOTO, O. 2001. Influence of particle size on the antibacterial activity of zinc oxide. *International Journal of Inorganic Materials,* 3**,** 643-646.

YOON, K.-Y., HOON BYEON, J., PARK, J.-H. & HWANG, J. 2007. Susceptibility constants of Escherichia coli and Bacillus subtilis to silver and copper nanoparticles. *Science of The Total Environment,* 373**,** 572-575.

YOU, Y., HAN, J., CHIU, P. C. & JIN, Y. 2005. Removal and Inactivation of Waterborne Viruses Using Zerovalent Iron. *Environmental Science & Technology,* 39**,** 9263-9269.

YUAN, X., PHAM, A. N., XING, G., ROSE, A. L. & WAITE, T. D. 2012. Effects of pH, Chloride, and Bicarbonate on Cu(I) Oxidation Kinetics at Circumneutral pH. *Environmental Science & Technology,* 46**,** 1527-1535.

ZHANG, Z. & EDWARDS, J. O. 1992. Chain lengths in the decomposition of peroxomonosulfate catalyzed by cobalt and vanadium. Rate law for catalysis by vanadium. *Inorganic Chemistry,* 31**,** 3514-3517.